

UNIVERSIDADE FEDERAL DO RIO GRANDE DO SUL

INSTITUTO DE QUÍMICA

LETICIA TODESCHINI

**ESTUDO FOTOFÍSICO DA INTERAÇÃO DE CIANINAS SIMÉTRICAS E  
ASSIMÉTRICAS COM A PROTEÍNA ALBUMINA SÉRICA BOVINA.**

Porto Alegre

2015

UNIVERSIDADE FEDERAL DO RIO GRANDE DO SUL

INSTITUTO DE QUÍMICA

LETICIA TODESCHINI

**ESTUDO FOTOFÍSICO DA INTERAÇÃO DE CIANINAS SIMÉTRICAS E  
ASSIMÉTRICAS COM A PROTEÍNA ALBUMINA SÉRICA BOVINA.**

Trabalho de conclusão apresentado junto à atividade de ensino “Trabalho de Conclusão de Curso - QUI” do Curso de Química, como requisito parcial para a obtenção do grau de Bacharel em Química.

Profa. Dra. Leandra F. Campo  
Orientadora

Porto Alegre

2015

Dedico este trabalho a minha família.

## **AGRADECIMENTOS**

Aos meus pais, Jussara e Luiz Angelo pelo suporte, auxílio, incentivo e amor por todos estes longos anos de faculdade.

A minhas irmãs Eliana e Gabriela.

Ao meu amigo e companheiro Leonardo, pela compreensão e cuidados.

Ao meu filhote Felipe, que foi o último empurrão para eu terminar a faculdade.

Aos colegas e agora amigos: Monique, Gabi, Carol, Karen, Jamili, Fabrício, Vane, Eric. Sem vocês o caminho teria sido impossível!

A professora Leandra, um exemplo de profissional, de orientadora e de mestre! Obrigada por ter me aceito como sua orientanda e ter sido tão paciente comigo!

## RESUMO

As cianinas vem sendo utilizadas nos últimos anos como sondas fluorescentes para detecção de proteínas em solução, pois mostram uma variação significativa na intensidade de fluorescência com a variação da concentração de proteína. Neste trabalho foi feito o estudo fotofísico da interação de cianinas simétricas e assimétricas com a albumina sérica bovina (BSA) em tampão fosfato (PBS). A partir da resposta fotofísica observada verificou-se que as cianinas assimétricas de cadeias longas se mostraram promissoras no objetivo de analisar quantitativamente as proteínas em meios biológicos, utilizando uma curva de calibração dos resultados de emissão de fluorescência.

**Palavras Chave:** Albumina Sérica Bovina (BSA), Cianinas, Fluorescência

## LISTA DE FIGURAS

FIGURA 1 - Estrutura tridimensional da Albumina Sérica Bovina (BSA) com os seus domínios (I-III) e subdomínios (A e B) representados.....	2
FIGURA 2 - Estruturas químicas das cianinas simétricas e assimétricas a serem estudadas por UV-Visível e Fluorescência na presença de BSA .....	3
FIGURA 3 - Espectros de absorção de UV-Visível e emissão de fluorescência em solução das cianinas 1-9 em PBS.....	7
FIGURA 4 - Espectro UV-Visível em solução das cianinas 5, 8 e 9 em diferentes concentrações de BSA (0-12 $\mu$ M).....	8
FIGURA 5 - Espectro de emissão de fluorescência em solução das cianinas 5, 8 e 9 em diferentes concentrações de BSA (0-12 $\mu$ M).....	10
FIGURA 6 - Curva de calibração para quantificação de BSA em PBS utilizando a cianina 8 como sensor óptico.....	12

## SUMÁRIO

<b>1 INTRODUÇÃO.....</b>	<b>1</b>
<b>2 OBJETIVO.....</b>	<b>4</b>
2.1 Objetivo Geral.....	4
2.2 Objetivos Específicos.....	4
<b>3 METODOLOGIA.....</b>	<b>5</b>
3.1 Preparo das Soluções .....	5
3.1.1 Tampão Fosfato PBS.....	5
3.1.2 BSA.....	5
3.1.3 Cianinas (1-9) .....	5
3.1.4 Conjugados cianinas (1-9)/BSA.....	5
3.2 UV-Visível e Fluorescência.....	6
<b>4 RESULTADOS E DISCUSSÃO.....</b>	<b>7</b>
4.1 Cianinas em PBS.....	7
4.2 Cianinas conjugadas a BSA.....	7
4.3 Quantificação da BSA por espectroscopia de fluorescência.....	11
<b>5. CONCLUSÕES.....</b>	<b>13</b>
<b>REFERÊNCIAS.....</b>	<b>14</b>
<b>APÊNDICES.....</b>	<b>15</b>
<b>ANEXO.....</b>	<b>21</b>

## 1. INTRODUÇÃO

As proteínas exercem inúmeras funções dentro do organismo, por isso o estudo de suas funções e atividades é muito importante para o desenvolvimento biotecnológico. Neste contexto, a albumina sérica bovina (BSA) é uma das proteínas mais utilizadas em estudos de associação com corantes.

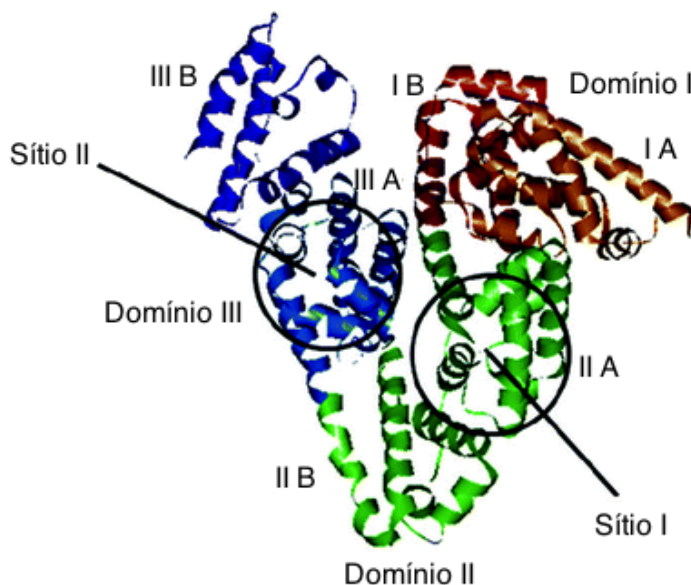
Albuminas séricas são as proteínas mais abundantes no plasma dos mamíferos, sendo que a BSA tem uma estrutura muito similar à albumina sérica humana (HSA). As albuminas são proteínas especialistas em encapsular moléculas que são insolúveis em água, tais como ácidos graxos, hormônios hidrofóbicos e fármacos liberando-os para uso pelas células de todo o corpo.

A BSA é uma proteína composta de três domínios estruturais similares (Figura 1, I-III), sendo que cada domínio contém dois subdomínios (Figura 1, A e B) estabilizados por 17 pontes de dissulfeto. Sabe-se que compostos aromáticos e heterociclos ligam-se aos sítios hidrofóbicos nos subdomínios IIA e IIIA, porém, uma dada molécula orgânica terá uma afinidade por um ou outro sítio dependendo da sua estrutura e do pH do meio.

Geralmente existem dois mecanismos de interação entre moléculas orgânicas e proteínas; a saber: (i) Interações Covalentes onde é necessário que a molécula tenha um grupo funcional reativo que se ligue a um grupo funcional reativo da proteína e (ii) Interações Não-Covalentes que ocorrem quando a molécula tem afinidade por áreas específicas da proteína. Aqui escolhemos investigar as interações entre uma classe de corantes conhecida como cianinas e a BSA.



Figura 1. Estrutura tridimensional da Albumina Sérica Bovina (BSA) com os seus domínios (I-III) e subdomínios (A e B) representados.



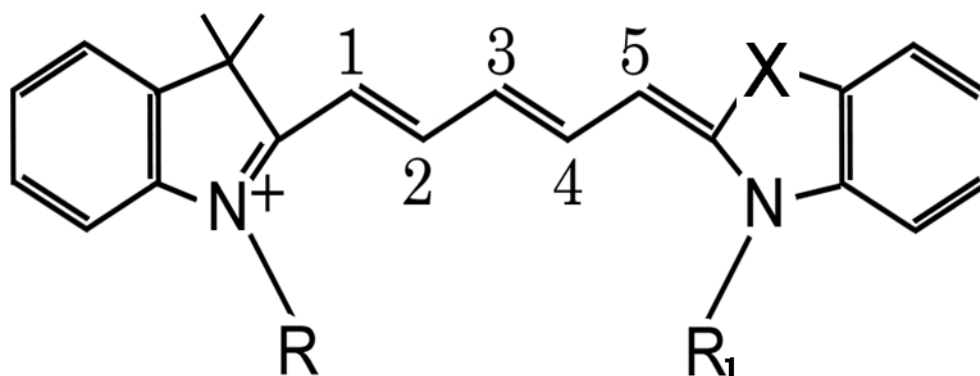
Fonte: Adaptado de <http://pubs.rsc.org/en/content/articlehtml/2012/ra/c2ra20633a>. Consultado em 18/10/2015.

As cianinas são compostos orgânicos fotossensíveis contendo dois anéis heterocíclicos com dois átomos de nitrogênio quaternizados que são ligados através de uma ponte polimetínica que consiste de múltiplos grupos  $\text{—HC=CH—}$  conjugados. Nos últimos anos, as cianinas têm sido usadas como sondas fluorescentes para a visualização de tecidos e células *in vivo* e *in vitro*, bem como na detecção e quantificação de proteínas em solução. As cianinas mostram grandes coeficientes de extinção molar e uma intensa absorção do tipo  $\pi\pi^*$  que pode ir desde a região do visível até o infravermelho próximo. Estas propriedades permitem que as cianinas sejam usadas em estudos de elucidação estrutural de proteína. Além disso, estes compostos têm uma elevada afinidade de ligação a ácidos nucleicos e, em geral, não são fluorescentes em água/tampão e só emitem fluorescência depois de interagir com uma biomolécula.

Neste trabalho realizamos o estudo por espectroscopia de absorção na região do UV-Visível e emissão de fluorescência das interações entre a proteína BSA e as cianinas simétricas (1-3) e assimétricas (4-9) (Figura 2) sintetizadas pelo Grupo de Fotoquímica

Orgânica do Instituto de Química desta Universidade. O trabalho apresentado faz parte de uma publicação recente do referido grupo. (Anexo A).

Figura 2. Estruturas químicas das cianinas simétricas e assimétricas a serem estudadas por UV-Visível e fluorescência na presença de BSA.



- 1- R=R<sub>1</sub>=etil, X=C(CH<sub>3</sub>)<sub>2</sub>
- 2- R=R<sub>1</sub>=butil, X=C(CH<sub>3</sub>)<sub>2</sub>
- 3- R=R<sub>1</sub>=octil, X=C(CH<sub>3</sub>)<sub>2</sub>
- 4- R=etil, R<sub>1</sub>=5-carboxipentil, X=C(CH<sub>3</sub>)<sub>2</sub>
- 5- R=etil, R<sub>1</sub>=5-carboxipentil, X=S
- 6- R=butil, R<sub>1</sub>=5-carboxipentil, X=C(CH<sub>3</sub>)<sub>2</sub>
- 7- R=butil, R<sub>1</sub>=5-carboxipentil, X=S
- 8- R=octil, R<sub>1</sub>=5-carboxipentil, X=C(CH<sub>3</sub>)<sub>2</sub>**
- 9- R=octil, R<sub>1</sub>=5-carboxipentil, X=S

## 2. OBJETIVOS

### 2.1. OBJETIVO GERAL

Estudar a interação da proteína BSA com as cianinas simétricas (**1-3**) e assimétricas (**4-9**) por espectroscopia de absorção na região do UV-Visível e emissão de fluorescência para fins de quantificação desta proteína em meios biológicos.

### 2.2. OBJETIVOS ESPECÍFICOS

- Preparar soluções de tampão fosfato (PBS) pH 7,4;
- Preparar soluções da proteína BSA em PBS pH 7,4;
- Preparar as soluções das cianinas simétricas (**1-3**) previamente sintetizadas em dimetilformamida na concentração de 14  $\mu$ M;
- Preparar as soluções das cianinas assimétricas (**4-9**) previamente sintetizadas em dimetilformamida na concentração de 14  $\mu$ M;
- Preparar as soluções das cianinas simétricas (**1-3**) com a proteína BSA;
- Preparar as soluções das cianinas assimétricas (**4-9**) com a proteína BSA;
- Realizar as medidas de absorção no UV-Visível dos conjugados cianinas/BSA;
- Realizar as medidas de fluorescência dos conjugados cianinas/BSA.

### 3. METODOLOGIA

#### 3.1. PREPARO DAS SOLUÇÕES

##### 3.1.1. Tampão Fosfato PBS

Foram pesados 8 g de NaCl (cloreto de sódio), 0,2 g de  $\text{KH}_2\text{PO}_4$  (monofosfato de potássio), 1,44 g de  $\text{Na}_2\text{HPO}_4$  (fosfato de sódio dibásico) e 0,2 g de KCl (cloreto de potássio), Os sólidos foram transferidos para um balão volumétrico com capacidade de 1 litro.

##### 3.1.2. BSA

A proteína utilizada foi a BSA Fração V obtida de Alamar Tecno-Científica LTDA, onde foram pesados 40,5 mg de BSA e misturar a 50 mL de PBS em balão volumétrico. A concentração final da solução foi de 14  $\mu\text{M}$ .

##### 3.1.3. Cianinas (1-9)

As cianinas 1-9 foram sintetizadas pelo Grupo de Fotoquímica Orgânica do Instituto de Química desta Universidade conforme literatura em anexo.

Foram preparadas soluções estoques das cianinas 1-9 pesando-se 2,5 mg do corante e dissolvendo-se em 5 mL de dimetilformamida para obter soluções com concentrações que variam de  $8,59 \times 10^{-4}$  a  $1,21 \times 10^{-3} \text{ M}^*$ .

##### 3.1.4. Conjugados cianinas (1-9)/BSA

Em 1 mL da solução de cianinas em PBS com concentração constante de 14  $\mu\text{M}$  foram adicionadas alíquotas de 0 a 6 mL da solução de BSA em PBS. O volume final foi completado Com PBS para atingir a faixa de concentração entre 0-12  $\mu\text{M}$  de proteína em solução. A mistura ficou sob agitação na temperatura ambiente durante 2 horas.

\*Alíquotas da solução mãe foram retiradas e diluídas até a obtenção da concentração final desejada da cianina a ser estudada.

Tabela 1- Volumes de cianina, BSA e PBS misturados para chegar na solução final de concentração de 0-12 $\mu$ M de Conjugados cianinas (1-9)/BSA.

Concentração final BSA( $\mu$ M)	cianina (mL)	BSA (mL)	PBS (mL)
0	1,0	0,0	6,0
1	1,0	0,5	5,5
2	1,0	1,0	5,0
3	1,0	1,5	4,5
4	1,0	2,0	4,0
5	1,0	2,5	3,5
6	1,0	3,0	3,0
7	1,0	3,5	2,5
8	1,0	4,0	2,0
9	1,0	4,5	1,5
10	1,0	5,0	1,0
11	1,0	5,5	0,5
12	1,0	6,0	0,0

### 3.2. UV-VISÍVEL E FLUORESCÊNCIA

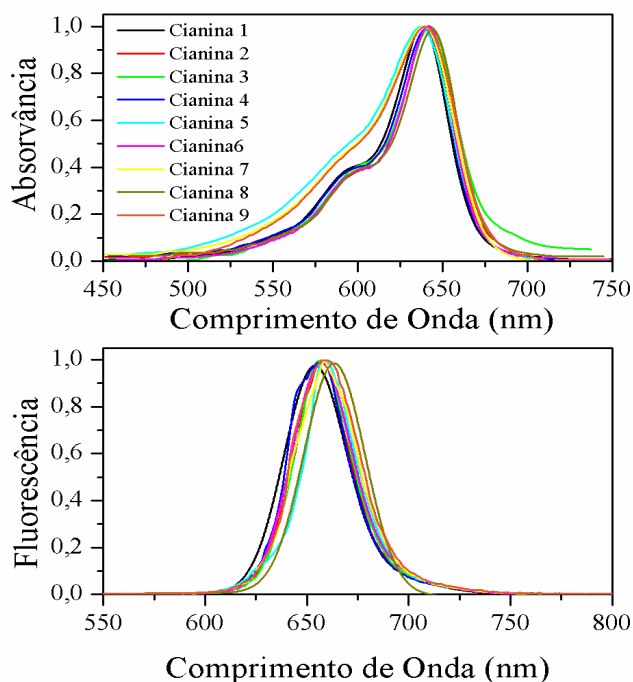
As soluções preparadas em 3.1.4 foram usadas para as medidas de absorção na região do UV-Visível e de fluorescência. Todas as medidas foram feitas a 25°C. Os espectros de absorção no UV-Visível foram realizados em equipamento Shimadzu UV-2450. Os espectros de emissão de fluorescência foram realizados em Shimadzu RF-5301PC.

## 4. RESULTADOS E DISCUSSÕES

### 4.1. CIANINAS EM PBS

O estudo fotofísico das cianinas foi feito em solução tampão PBS. Pode-se observar que nem as variações estruturais como a quaternização por grupos etil, butil ou octil, nem o fato de serem simétricas ou não afetaram o comportamento fotofísico das cianinas 1-9 onde o máximo de absorção localizou-se aproximadamente em 640nm e o máximo de emissão em 660nm. Além disso na Figura 3 observamos pelos espectros de absorção no UV-Visível e de Fluorescência das cianinas 1-9 em tampão PBS que todos os espectros apresentam o mesmo perfil.

Figura 3: Espectros de absorção de UV-Visível e emissão de fluorescência em solução das cianinas 1-9 em PBS.



### 4.2. CIANINAS CONJUGADAS A BSA

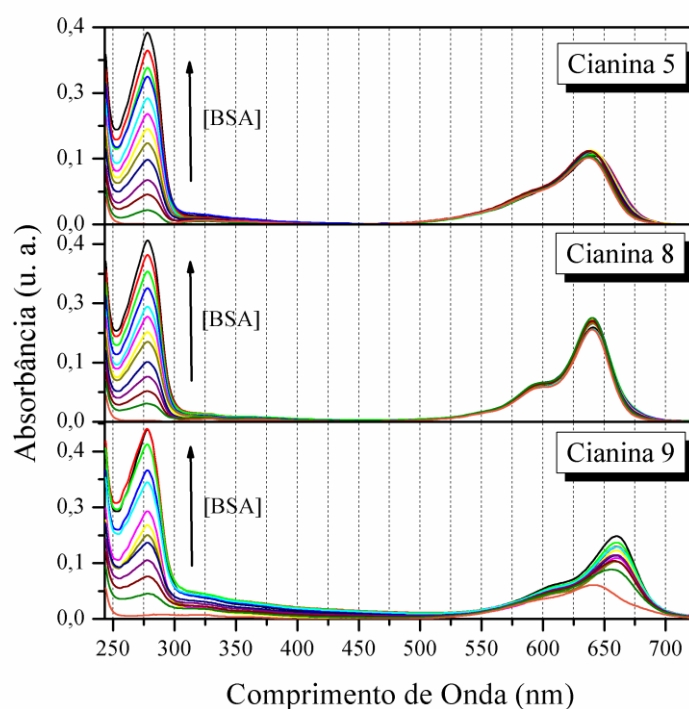
O estudo fotofísico das cianinas e dos respectivos conjugados foi realizado em PBS e está sumarizado na Tabela 2 onde se percebe um leve deslocamento na localização do máximo de absorção e de fluorescência devido à interação das cianinas com a BSA.

Tabela 2- Dados fotofísicos de absorção de UV-Visível e de fluorescência das soluções das cianinas 1-9 em PBS e em PBS/BSA.

Cianina	PBS		PBS/BSA	
	$\lambda_{Abs.}$	$\lambda_{Em.}$	$\lambda_{Abs.}$	$\lambda_{Em.}$
1	638	655	637	655
2	638	658	637	664
3	644	658	649	670
4	640	655	640	657
5	639	659	630	662
6	643	658	640	658
7	639	659	643	673
8	640	655	640	666
9	642	660	660	678

Na figura 4 podem ser observados os espectros na região do UV-Visível das cianinas 5, 8 e 9 na presença de BSA que mostraram a banda característica da BSA em torno de 270 nm<sup>14</sup> e a das cianinas em torno de 637 nm. Pode-se observar que as cianinas mantiveram suas propriedades de absorção mesmo conjugada com a BSA.

Figura 4: Espectro UV-Visível em solução das cianinas 5, 8 e 9 em diferentes concentrações de BSA (0-12  $\mu$ M).



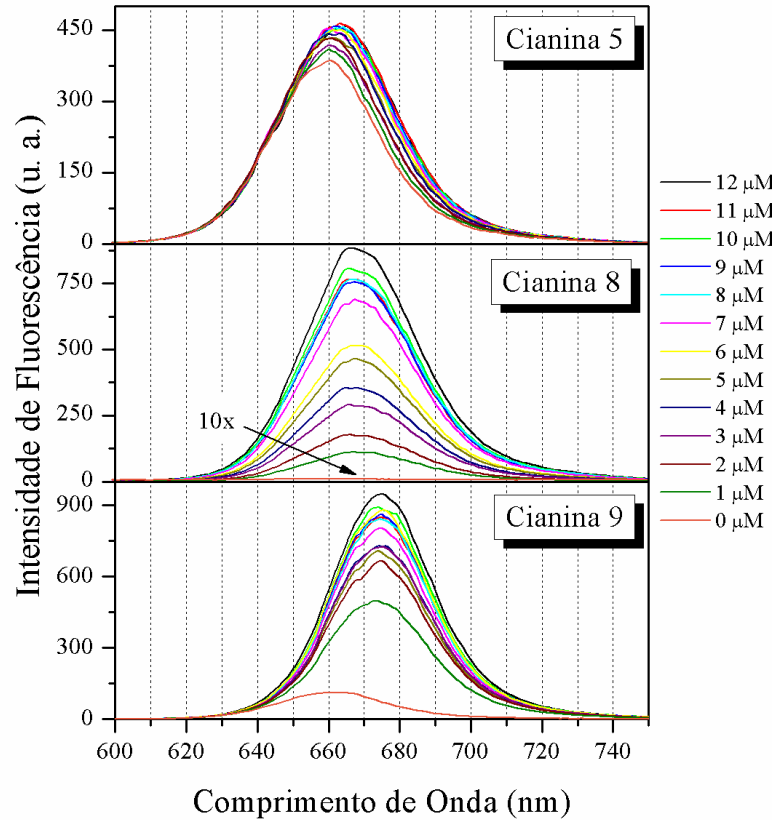
Os espectros da Figura 4 mostram dois conjuntos distintos de curvas, que podem ser relacionadas com regiões de absorção da BSA (250-300 nm) e da cianina (500-700 nm). Pode-se observar que com aumento de BSA aumentou a intensidade de absorção entre 250-300 nm, como esperado. No entanto, considerando a região das cianinas, foram observados dois comportamentos distintos. Independente da quantidade de BSA, as cianinas 5 e 8 apresentaram absorção em cerca de 637 nm com uma intensidade quase constante. Apesar da absorção intensa na ausência de BSA, a cianina 9 aumentou a intensidade de absorbância após a adição de BSA, embora haja na literatura que com a adição de proteína ocorra uma queda inicial na absorção máxima devido a formação dos agregados seguida por um gradual acréscimo dessa intensidade após a ruptura dos agregados chegando próximo ao valor inicial<sup>1</sup>. Além disso, a BSA em solução desloca os máximos de absorção em 25 nm para o vermelho, como já observado para estruturas semelhantes. O máximo de absorção observado para a cianina 9 na presença de BSA pode ser provavelmente relacionado com o conjugado BSA/cianina no estado fundamental. As pequenas alterações na intensidade de absorção da radiação UV-Visível e os máximos para as cianinas 5 e 8 na presença de BSA não descartam a presença de conjugados em solução.

A BSA é uma proteína globular composta por três domínios estruturalmente semelhantes, cada uma contendo dois subdomínios (A e B) e estabilizadas por 17 pontes de dissulfeto<sup>2-6</sup>. Sabe-se que aromáticos e ligantes heterociclos são encontrados ligados com dois sítios hidrofóbicos em subdomínios II e III, nomeados sítio I e o sítio II<sup>2-7</sup>. Na BSA, foi sugerido que as cianinas apresentam uma especificidade elevada para o subdomínio III A (sítio II)<sup>8-11</sup>. Embora na literatura esteja presente que a afinidade de ligação de algumas cianinas não é somente dependente da hidrofobicidade, mas pode ser influenciada por interferências estéricas dentro dos sítios de ligação<sup>11</sup>, existe um esquema geral que com o aumento da hidrofobicidade entre cianinas aumenta de afinidade de ligação com a BSA. Desta forma, a comparação dos dados de UV-Visível da série das cianinas estudadas pôde-se supor que o aumento das cadeias alquil leva a um aumento da afinidade do corante com a BSA no estado fundamenta<sup>12-13</sup>. Além disso, vale ressaltar que o mesmo comportamento foi observado para todos os corantes sintetizados com estrutura química similar.

Na figura 5 observa-se que as cianinas mantêm suas propriedades de emissão em torno de 650 nm e que ocorre a conjugação entre a cianinas e a BSA, pois há uma variação na quantidade de emissão de fluorescência com a variação da concentração de BSA.



Figura 5: Espectro de emissão de fluorescência em solução das cianinas 5, 8 e 9 em diferentes concentrações de BSA (0-12  $\mu\text{M}$ ).



As características dos espectros de emissão de fluorescência das cianinas 5, 8 e 9 na ausência e presença de BSA são apresentados na Figura 5. As curvas adicionais dos corantes 1, 2, 3, 4, 6 e 7 são apresentados no Apêndice B.

Na Figura 5 observa-se que as cianinas utilizadas no estudo não apresentaram novas bandas de emissão de fluorescência devido a agregados em solução, apesar dos corantes cianinas da literatura terem apresentado<sup>13-14</sup>. Sensores ópticos para detectar proteína em solução geralmente apresentam agregados não fluorescentes, que na presença de proteína aumentam a emissão de fluorescência do corante devido à ruptura destes agregados não fluorescentes. No entanto, as cianinas relatadas neste trabalho se comportam de maneira diferente. A cianina 5 apresenta uma emissão de fluorescência significativa em PBS pois não forma esses agregados que só se rompem após a interação. Além disso, não pôde ser observada uma correlação linear entre a intensidade de fluorescência e a concentração de proteína. Os mesmos resultados foram observados para as cianinas 1, 2, 4 e 6. Por outro lado, as cianinas 3, 7, 8 e 9 apresentaram uma intensidade de fluorescência que aumentou com a

quantidade de BSA em solução. As cianinas 3, 7 e 9 apresentaram fluorescência na ausência de BSA. A primeira adição de BSA (1  $\mu\text{M}$ ) aumentou a emissão de fluorescência de 2-4 vezes. Após a última adição de proteína (12  $\mu\text{M}$ ) a fluorescência aumentou de quatro até oito vezes, dependendo da cianina, assim como os máximos de emissão foram deslocados em torno de 20 nm para o vermelho. O desvio batocrômico observado sugere que os microambientes BSA são menos polares do que o PBS devido aos grupos hidrófobos presentes na superfície e no interior da BSA. Além disso, a cianina 8 foi quase não-fluorescente na ausência de BSA e aumentou de intensidade de fluorescência 50 até 450 vezes após a adição de 1 e 12  $\mu\text{M}$  de BSA, respectivamente. Este resultado indica que a cianina 8 apresentou uma afinidade mais elevada com a BSA devido ao carácter mais hidrofóbico da combinação de cadeia alquil longa com os grupos metil presentes no anel indoleninium.

#### **4.3. QUANTIFICAÇÃO DA BSA POR ESPECTROSCOPIA DE FLUORESCÊNCIA**

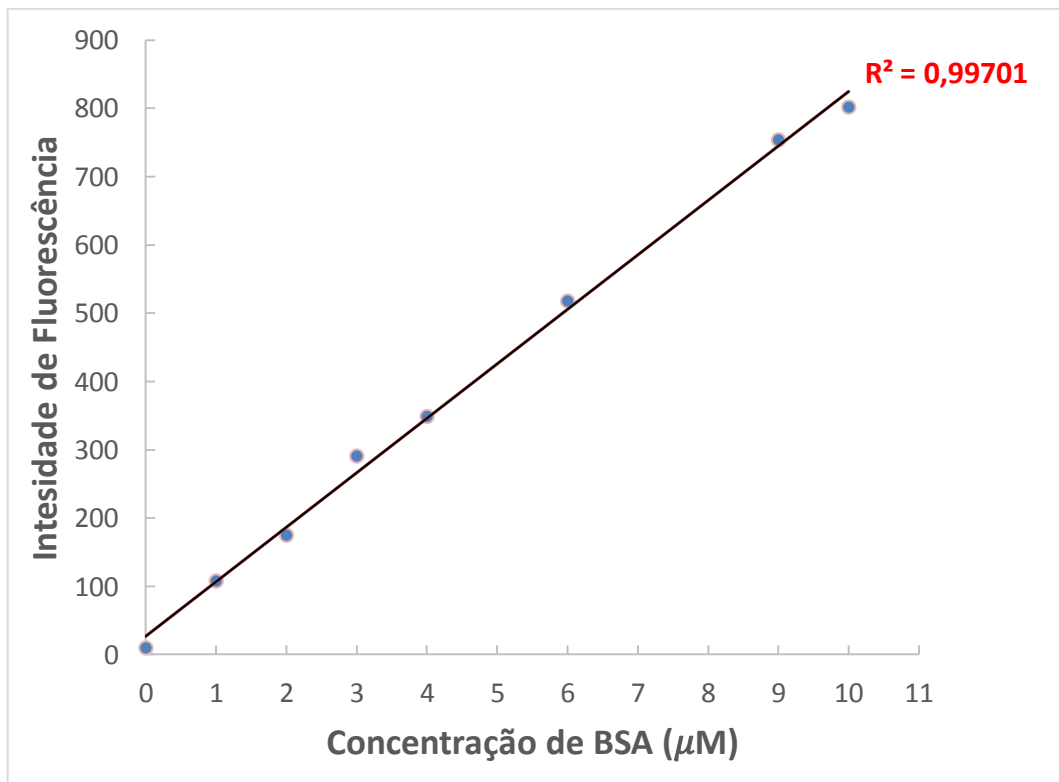
Foram avaliadas as intensidades de fluorescência das cianinas simétricas e assimétricas, não se obteve resultados satisfatórios para as cianinas simétricas e as cianinas assimétricas de cadeias curtas. Os resultados mostram que com a cianina 8 se obteve um bom resultado para fins de quantificação de proteínas em solução. Na figura 6 podemos ver que o coeficiente de correlação encontrado foi de 0,99071 confirmando que a cianina 8 pode ser utilizada para fins de qualificação de proteínas. A curva de calibração foi somente uma aproximação, apesar de ter dado resultado positivo, para utilizar esse método com garantias seria necessário refazer as soluções de cianina 8 e as medidas de fluorescência em no mínimo 3 vias para ter valores mais corretos e utilizar métodos estatísticos de análise.

Na tabela 3 observa-se que há um aumento gradativo da intensidade de fluorescência com o aumento da concentração para a cianinas assimétricas e de cadeias longas 8 e 9. Já para a cianina 5 (assimétrica de cadeia curta) os valores da intensidade de fluorescência se mostraram muito próximos, não variam com a concentração de BSA, assim como as demais cianinas assimétricas de cadeias curtas 4-7 e as simétricas 1-3 (Apêndice B).

Tabela 3- Dados de intensidade de fluorescência em relação a concentração de BSA das cianinas 5, 8 e 9.

Concentração BSA ( $\mu\text{M}$ )	Intensidade de emissão da cianinas 5	Intensidade de emissão da cianinas 8	Intensidade de emissão da cianinas 9
0	383	10	81
1	407	108	496
2	429	175	663
3	416	291	727
4	439	349	728
5	433	466	707
6	448	518	874
7	450	680	806
8	455	763	840
9	442	754	860
10	451	802	891
11	463	763	857
12	459	879	942

Figura 6 – Curva de calibração para quantificação de BSA em PBS utilizando a cianina 8 como sensor óptico.



## 5. CONCLUSÕES

Observou-se que as cianinas que contêm cadeias mais longas e assimétricas mostram uma melhor variação de intensidade de fluorescência na presença de BSA. Dentre as cianinas utilizadas no estudo a cianina 5 que é assimétrica e de cadeia curta, não mostrou linearidade com aumento da intensidade de fluorescência, a cianina 8 assimétrica e de cadeia longa obteve o melhor resultado chegando a um coeficiente de correlação de 0,99701 e ainda mostrou-se pouco fluorescente na ausência de BSA devido a formação de agregados em solução e com a primeira adição de BSA aumentou em 50 vezes a intensidade de fluorescência, a cianina 9 apesar de ser assimétrica e de cadeia longa, tem o enxofre que torna a molécula mais polar o que torna a interação mais difícil, pois o sítio da BSA é mais apolar.

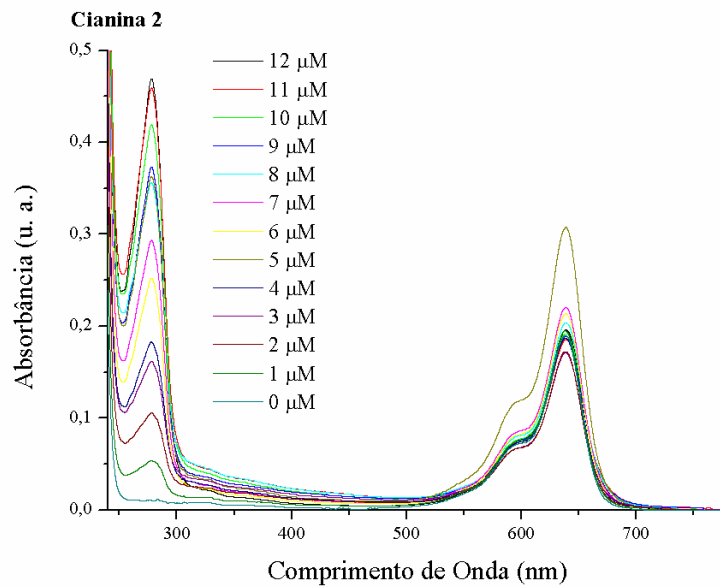
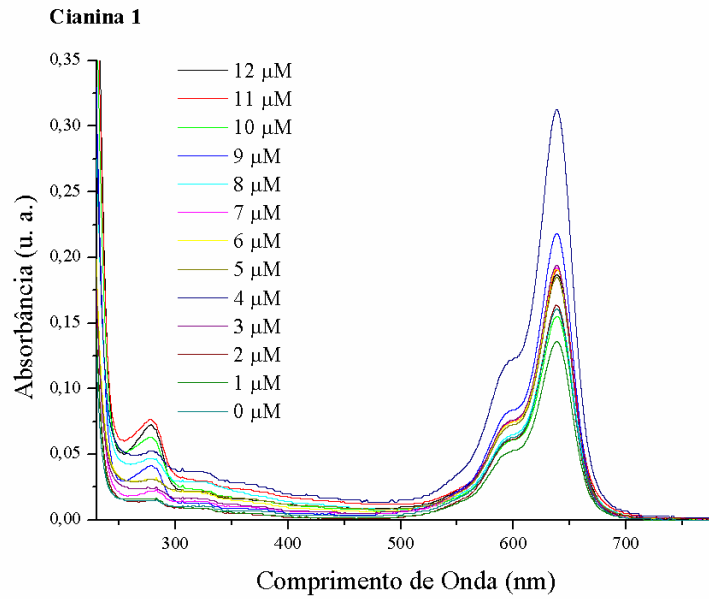
A cianina 8 é indicada na análise quantificação de BSA para a faixa de concentração de 0-12 $\mu$ M de BSA em solução a 2  $\mu$ M de cianina.

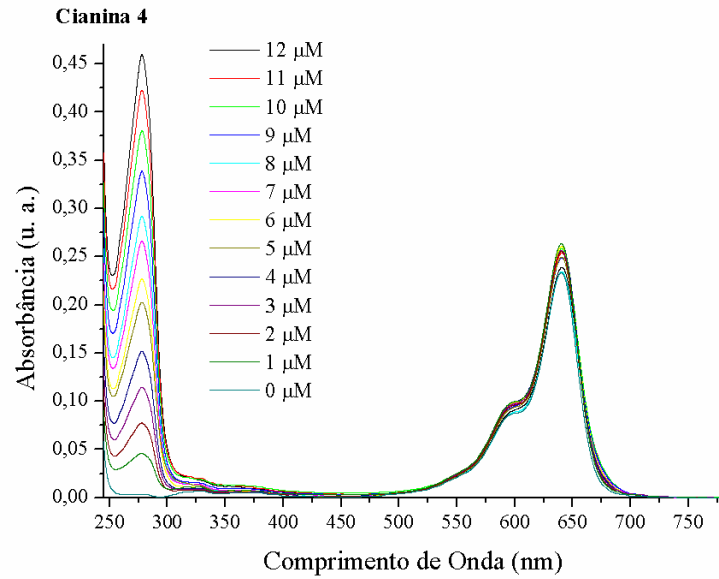
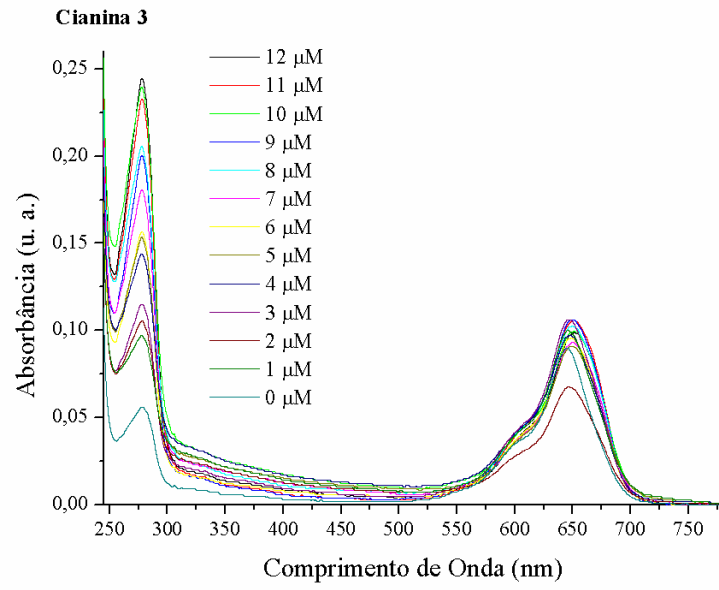
## REFERÊNCIAS

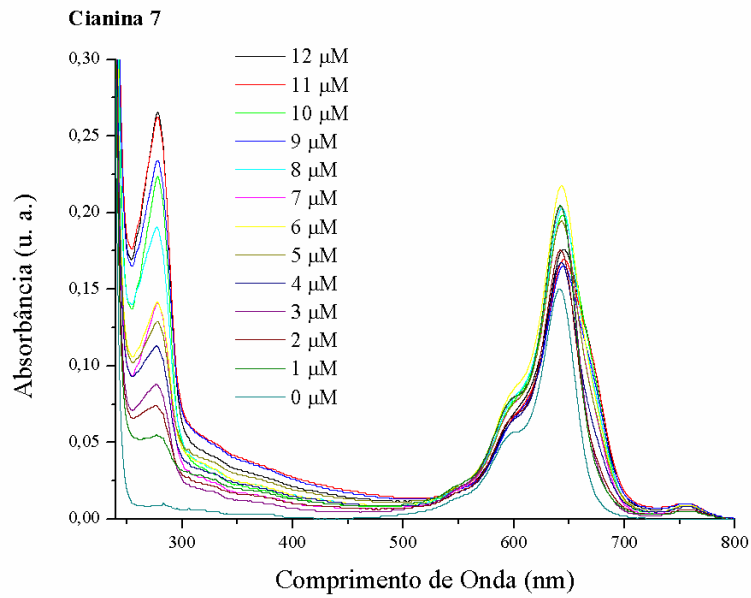
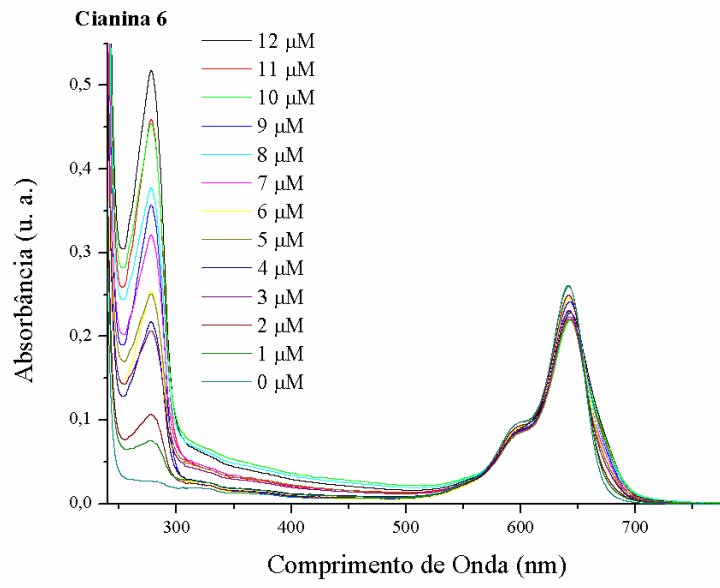
- (1) Tatikolov; A. S.; Costa; S. M. B. *Biophys. Chem.* **2004**, 107, 33.
- (2) Fujimoto; Y.; Katayama; N.; Ozaki; Y.; Yasui; S.; Iriyama, K. *J. Mol. Struct.* **1992**, 274, 183.
- (3) Ilharco; L. M.; de Barros; R. B. *Langmuir* **2000**, 16, 9331
- (4) Steiger; R.; Pugin; R.; Heier; J. *Colloids Surf. B* **2009**, 74, 484.
- (5) Khairutdinov; R. F.; Serpone; N. *J. Phys. Chem. B* **1997**, 101, 2602.
- (6) Gadde; S.; Batchelor; E. K.; Kaifer; A. E. *Chem. Eur. J.* **2009**, 15, 6025.
- (7) West; W.; Pearce; S. *J. Phys. Chem.* **1965**, 69, 1894.
- (8) Kovalska; V. B.; Volkova; K. D.; Manaev; A. V.; Losytskyy; M. Y.; Okhrimenko; I. N.; Traven; V. F.; Yarmoluk; S. M. *Dyes Pigment.* **2010**, 84, 159.
- (9) Tatikolov; A. S. *J. Photochem. Photobiol. C Photochem. Rev.* **2012**, 13, 55.
- (10) Carter; D. C.; Ho; J. X. *Adv. Prot. Chem.* **1994**, 45, 153.
- (11) He; H. M.; Carter; D. C. *Nature* **1992**, 358, 209.
- (12) Peters; T. *All about Albumin: Biochemistry; Genetics; and Medical Applications*; Academic Press; Berlin, **1996**.
- (13) Curry; S.; Brick; P.; Frank; N. P. *Biochim. Biophys. Acta* **1999**, 1441, 131.
- (14) Abassi; P.; Abassi; F.; Yari; F.; Hashemi; M.; Nafisi; S. *J. Photochem. Photobiol. B Biol.* **2013**, 122, 61.

## APÊNDICES

**APÊNDICE A** - Espectro de absorção no UV-Visível das cianinas 1-4, 6 e 7 em diferentes concentrações de BSA [0-12  $\mu\text{M}$ ].

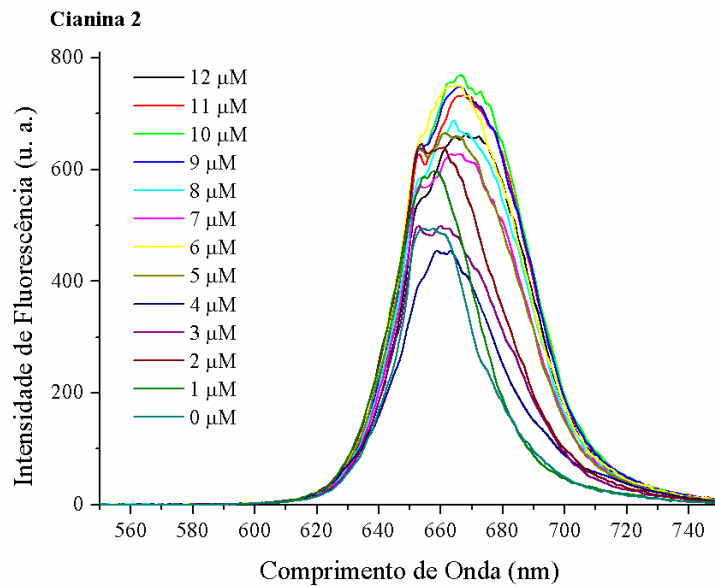
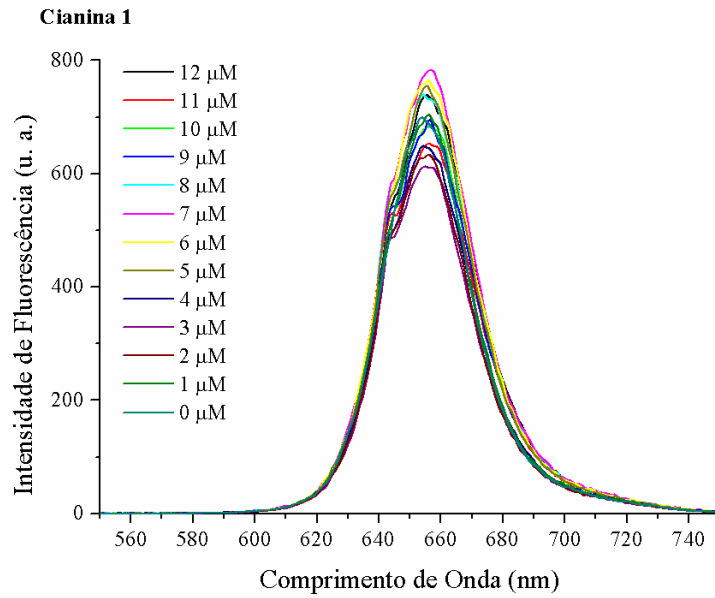


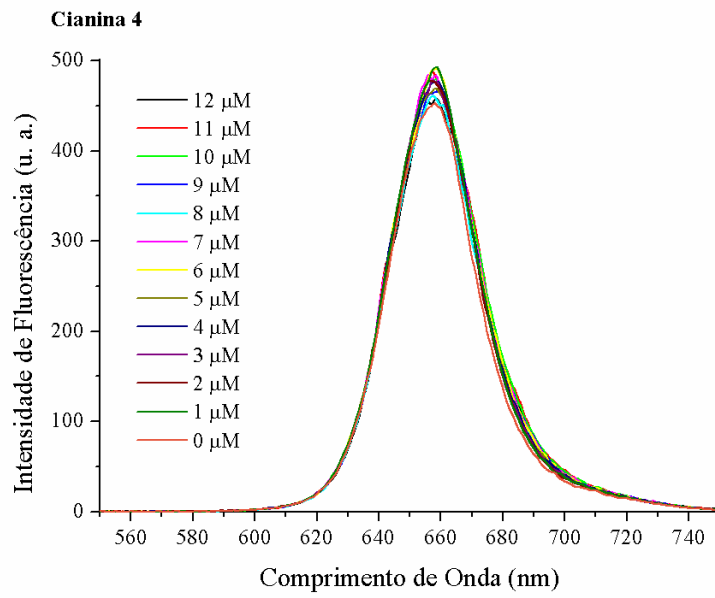
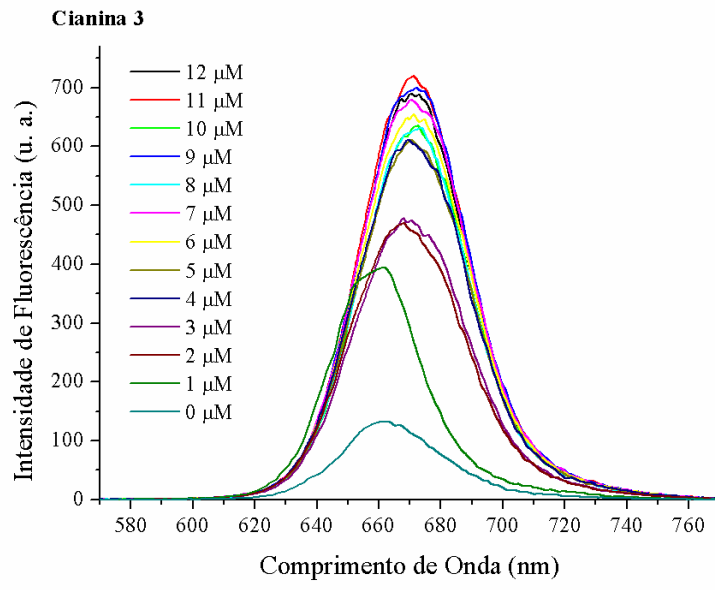


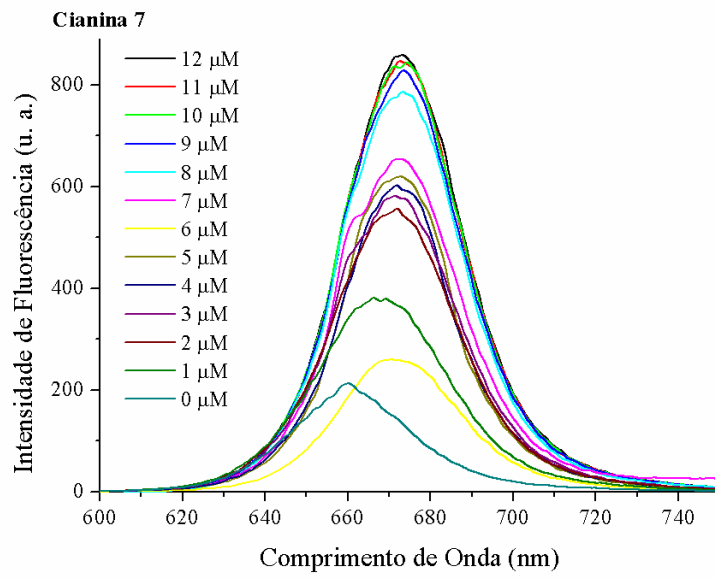
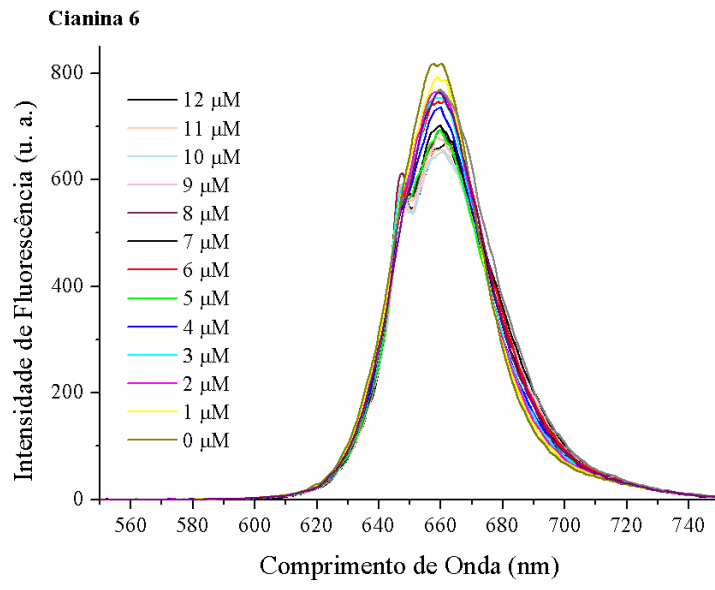




**APÊNDICE B** - Espectro de emissão de fluorescência das cianinas 1-4, 6 e 7 em diferentes concentrações de BSA [0-12  $\mu\text{M}$ ].







## ANEXO

PUBLICAÇÃO DO GRUPO DE FOTOQUÍMICA ORGÂNICA DO INSTITUTO DE QUÍMICA DESTA  
UNIVERSIDADE.

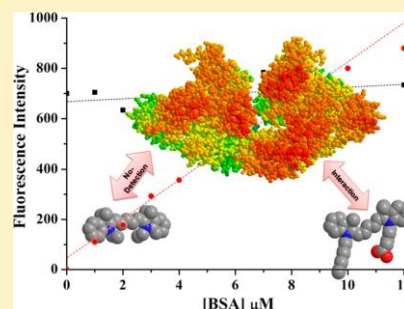
## Symmetrical and Asymmetrical Cyanine Dyes. Synthesis, Spectral Properties, and BSA Association Study

Diego S. Pisoni, Leticia Todeschini, Antonio César A. Borges, Cesar L. Petzhold, Fabiano S. Rodembusch,<sup>\*,†</sup> and Leandra F. Campo<sup>\*</sup>

Instituto de Química, Universidade Federal do Rio Grande do Sul, Avenida Bento Gonçalves, 9500, CP 15003. CEP 91501-970, Porto Alegre-RS, Brazil

Supporting Information

**ABSTRACT:** New cyanines were prepared by an efficient and practical route with satisfactory overall yield from low-cost starting materials. The photophysical behavior of the cyanines was investigated using UV-vis and steady-state fluorescence in solution, as well as their association with bovine serum albumin (BSA) in phosphate buffer solution (PBS). No cyanine aggregation was observed in organic solvents or in phosphate buffer solution. The alkyl chain length in the quaternized nitrogen was shown to be fundamental for BSA detection in PBS in these dyes.

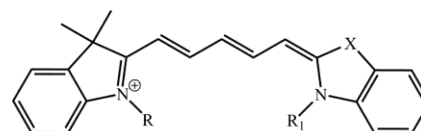


### INTRODUCTION

Cyanine dyes are photosensitive structures composed of two quaternized nitrogen-containing heterocyclic ring structures that are linked through a polymethine bridge.<sup>1</sup> In recent years, cyanine dyes have been used as fluorescent probes in biomedical screening techniques,<sup>2–4</sup> luminescent materials for labeling,<sup>5–8</sup> and analyte responsive fluorescent probes<sup>9</sup> in optoelectronic applications.<sup>10–12</sup> Cyanines show large extinction coefficients and an intense  $^1\pi\pi^*$  absorption which can be easily tuned from the visible to the NIR region by structural modifications in the chromophore moiety.<sup>13</sup> This property allows the cyanines to be designed in order to achieve the desired functional fluorescent nanomaterials, for instance, in DNA studies,<sup>14–16</sup> as well as in biological applications.<sup>17</sup> Furthermore, cyanine dyes have a high binding affinity to nucleic acids and usually are nonfluorescent in water/buffer; however, they emit fluorescence only after binding to a substrate.

Cyanine dyes can also be used in biological applications due to their absorption and fluorescence features. The large range of their fluorescence spectra and good fluorescence quantum yield enables the detection of low concentrations of analytes.<sup>18</sup> Moreover, they can be employed as FRET acceptors,<sup>19–22</sup> improving energy transfer between donor and acceptor and reducing the background noise during real time polymerase chain reaction experiments.

This paper describes the detailed synthesis and the spectroscopic characterization of the indolium- and benzothiazolium-based pentamethine cyanine dyes 1–9 with *N*-alkyl (ethyl, butyl, and octyl) and *N*-(5-carboxypentyl) groups (Figure 1). In addition, the photophysical study of these



- 1, R = R<sub>1</sub> = ethyl, X = C(CH<sub>3</sub>)<sub>2</sub>
- 2, R = R<sub>1</sub> = butyl, X = C(CH<sub>3</sub>)<sub>2</sub>
- 3, R = R<sub>1</sub> = octyl, X = C(CH<sub>3</sub>)<sub>2</sub>
- 4, R = ethyl, R<sub>1</sub> = 5-carboxypentyl, X = C(CH<sub>3</sub>)<sub>2</sub>
- 5, R = ethyl, R<sub>1</sub> = 5-carboxypentyl, X = S
- 6, R = butyl, R<sub>1</sub> = 5-carboxypentyl, X = C(CH<sub>3</sub>)<sub>2</sub>
- 7, R = butyl, R<sub>1</sub> = 5-carboxypentyl, X = S
- 8, R = octyl, R<sub>1</sub> = 5-carboxypentyl, X = C(CH<sub>3</sub>)<sub>2</sub>
- 9, R = octyl, R<sub>1</sub> = 5-carboxypentyl, X = S

**Figure 1.** Chemical structure of the symmetrical and asymmetrical cyanine dyes.

compounds was performed in organic solvents and in buffer solution. Their potential application as fluorescent probes to detect protein in phosphate buffer solution (PBS) was also explored using bovine serum albumin (BSA) as a model, since the interaction of these dyes with proteins has been studied in less detail in comparison with that for nucleic acids.<sup>23</sup>

### RESULTS AND DISCUSSION

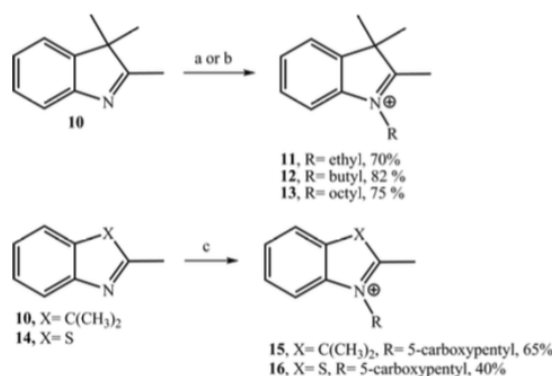
**Synthesis of Quaternary Heterocyclic Ammonium Salt Precursors.** The heterocyclic ammonium salts were synthesized by quaternization of the corresponding hetero-

Received: March 22, 2014

Published: May 20, 2014

aromatic base 2,3,3-trimethylindolenine (**10**) or 2-methylbenzothiazole (**14**) with suitable alkylating agents such as alkyl halides or 6-bromohexanoic acid, in the presence or absence of solvent.<sup>24,25</sup>

*N*-Ethyl-2,3,3-trimethylindoleninium bromide (**11**) was prepared by the condensation of 2,3,3-trimethylindolenine (**10**) with 2.0 equiv of bromoethane, at 120 °C in *o*-dichlorobenzene for 24 h (Scheme 1). The resulting

Scheme 1. <sup>a</sup>

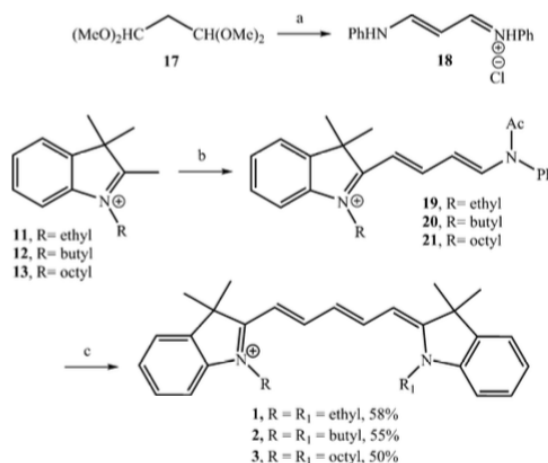
<sup>a</sup>Reagents and conditions: (a) bromoethane, *o*-dichlorobenzene, 120 °C, 24 h, for **11**; (b) 1-iodoalkane, 145 °C, 3 h, for **12** and **13**; (c) 6-bromohexanoic acid, *o*-dichlorobenzene, 120 °C.

ammonium salt **11** was readily separated in high purity from the crude reaction mixture by precipitation upon addition of hexane and diethyl ether and isolated in 70% yield after filtration. The salts *N*-butyl-2,3,3-trimethylindoleninium iodide (**12**) and *N*-octyl-2,3,3-trimethylindoleninium iodide (**13**) were prepared by heating solutions containing **10** and an excess (5.0 equiv) of 1-iodobutane or 1-iodooctane, respectively, in the absence of solvent at 145 °C (Scheme 1).<sup>26</sup> After purification by chromatography, the unreacted amount of alkylating agent was recovered and the precursors **12** and **13** were obtained in 82% and 75% yields, respectively.

Although many reports on the synthesis of heterocyclic ammonium salts use reflux  $\times$  with a large excess of organic solvent (usually acetonitrile) over several days and without further purification,<sup>27,28</sup> it was decided to synthesize these derivatives using a solvent-free approach. This procedure allowed us to minimize the reaction time to a few hours. However, considering that the condensation reaction involves temperatures above 80 °C, this methodology could not be applied to prepare the precursor **11** due to the low boiling point (38 °C) of bromoethane.

1-(5-Carboxypentyl)-2,3,3-trimethyl-indoleninium bromide (**15**) was obtained by the coupling of 2,3,3-trimethylindolenine (**10**) with 1.2 equiv of 6-bromohexanoic acid at 120 °C in *o*-dichlorobenzene for 24 h (Scheme 1).<sup>29</sup> According to this procedure, the precursor **15** was obtained in good yield (65%) after purification by chromatography. Similarly, 3-(5-carboxypentyl)-2-methylbenzo[d]thiazol-3-ium bromide (**16**) was prepared by the condensation of 2-methylbenzothiazole (**14**) with 6-bromohexanoic acid (Scheme 1). The resulting ammonium salt **16** was separated in 40% yield in high purity from the crude reaction mixture by precipitation upon addition of hexane and diethyl ether.

**Synthesis of the Cyanine Dyes.** The synthetic route to symmetrical and unsymmetrical cyanine dyes involves the condensation of cationic heterocyclic compounds containing an activated methyl group with derivatives of malondialdehyde. For the synthesis of cyanine dyes **1–9**, initially the three-carbon spacer precursor **18** was prepared from the commercially available 1,1,3,3-tetramethoxypropane (**17**) (Scheme 2). The condensation reaction between **17** and aniline, under acidic conditions, yielded the benzenaminium chloride **18** in 85% yield after isolation by precipitation.<sup>30</sup>

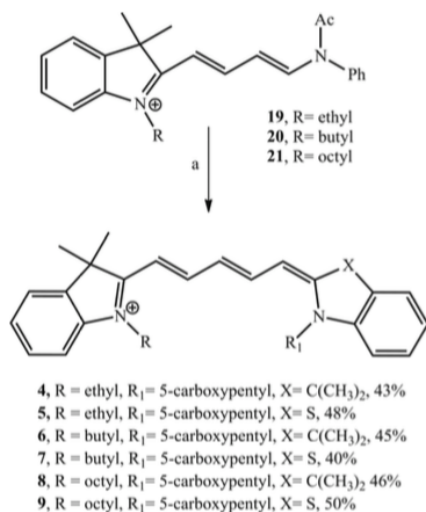
Scheme 2. <sup>a</sup>

<sup>a</sup>Reagents and conditions: (a) PhNH<sub>2</sub>, aqueous HCl, 50 °C, 85%; (b) **18**, Ac<sub>2</sub>O, 125 °C, 2 h; (c) **11–13**, NaOAc, EtOH, reflux, 6 h.

The symmetrical cyanines **1–3** were synthesized in two steps from de alkyl quaternized salts **11–13** through activated intermediates **19–21**, according to the synthetic pathway described in Scheme 2. The acetylated precursors **19–21** were prepared by the reaction of equimolar amounts of the corresponding *N*-alkylammonium salt **11–13** and the precursor **18** under reflux in Ac<sub>2</sub>O over 2 h.<sup>31</sup> It is worth mentioning that intermediates **19–21** were obtained in good purity according to the <sup>1</sup>H NMR analysis of each crude product and were used without further purification in the second step. Next, a condensation reaction between the crude products containing mainly the *N*-acyl precursors **19–21** and 1.0 equiv of quaternized salts **11–13**, in the presence of NaOAc and under reflux in EtOH over 6 h, afforded the symmetrical cyanines **1–3** in satisfactory yields after purification by chromatography.

In a similar way, the asymmetrical cyanines **4–9** containing a *N*-carboxypentyl group were synthesized as depicted in Scheme 3. The asymmetrical dyes were prepared by condensation between the precursors **15** or **16** and the activated intermediates **19–21**, in the presence of NaOAc and under reflux in EtOH over 3 h. According to this procedure, dyes **4–9** were obtained in good yields after purification by chromatography and no esterification products of the carboxyl group were observed.

It is worth mentioning that asymmetric cyanine dyes have gained much interest due to their excellent nucleic acid staining properties.<sup>32</sup> Upon binding to nucleic acids, asymmetric

Scheme 3. <sup>a</sup>

<sup>a</sup>Reagents and conditions: (a) 15 or 16, NaOAc, EtOH, reflux, 3 h.

cyanine dyes usually exhibit a large enhancement in fluorescence intensity;<sup>33</sup> they are widely used as fluorescent markers for DNA in various contexts.<sup>34–36</sup>

**Spectroscopic Characterization.** Analysis of the FTIR spectra allowed us to distinguish between the absorption bands from the chromophore and the aliphatic chains. Figure 2 depicts an expansion of the FTIR spectra for the cyanines 4–9 between 800 and 1800 cm<sup>-1</sup>. The full FTIR spectra of the cyanines 1–9 are presented in the Supporting Information. The two bands located around 2920 and 2860 cm<sup>-1</sup> were assigned to CH<sub>2</sub> asymmetric and symmetric stretching modes of the hydrocarbon chains. Additionally, the band at 2960 cm<sup>-1</sup> (data not shown) was attributed to an asymmetric stretching mode of CH<sub>3</sub> groups. The infrared absorption bands at 1720 cm<sup>-1</sup> were assigned to C=O stretching from the 5-carboxy group at the end of the alkyl chain. Vibrational assignments in the region between 1600 and 1380 cm<sup>-1</sup> were related to the stretching and deformation modes of the resonant central chain of the cyanine dyes.<sup>37,38</sup> The positions and relative intensities of the bands related to the central chain are consistent with an all-trans conformation, which has been well established for a variety of cyanine dyes.<sup>38</sup> In general, the symmetrical as well as the asymmetrical cyanine dyes do not show considerable differences in the FTIR spectra. Significant changes were found for the asymmetric cyanines 5, 7, and 9, which present a sulfur atom in the backbone, presenting a more intense absorption band at 1570 cm<sup>-1</sup> which can be related to the indolenine C=N stretching in comparison to that in the parent compounds.<sup>39</sup> Additionally, these sulfur derivatives presented an absorption band between 1500 and 1450 cm<sup>-1</sup>. It is also worth mentioning that the observed absorption bands at 1330–1070 cm<sup>-1</sup> may be attributed to the stretching modes or to the CH in-plane deformation modes of the central conjugated systems, since phenyl rings do not usually have prominent bands at 1400–1100 cm<sup>-1</sup>.

It is worth mentioning that the <sup>1</sup>H and <sup>13</sup>C NMR spectra of symmetrical and asymmetrical cyanines are quite different. The asymmetrical dyes have split signals in the <sup>1</sup>H and <sup>13</sup>C NMR in contrast to the symmetrical dyes, mainly the cyanines 5, 7, and

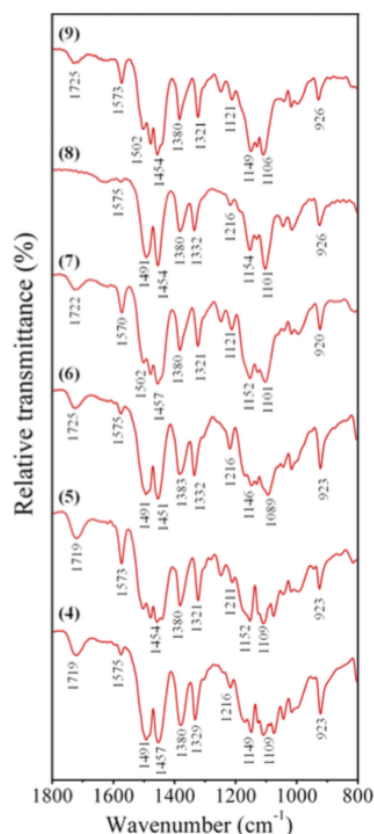


Figure 2. FTIR spectra of the cyanines 4–9: expansion from 800 to 1800 cm<sup>-1</sup>.

9, which show, for example, two signals to each CH<sub>2</sub> attached to the nitrogen of the indolenine ring (Supporting Information, Figures S30, S38, and S46).

**Photophysical Characterization.** The photophysical study was performed in solutions of chloroform, dimethylformamide (DMF), ethanol, and dimethyl sulfoxide (DMSO). The relevant data are summarized in Table 1. Figure 3 depicts the UV–vis absorption and fluorescence emission spectra from the symmetrical cyanines 1–3 in chloroform and dimethylformamide. It can be observed that the maxima locations (absorption and emission) as well as the curve shapes were not affected by the alkyl moiety present in these compounds (ethyl, butyl, and octyl). A very similar behavior was observed in ethanol and DMSO (Supporting Information). Absorption band maxima located around 650 nm with high molar absorption coefficient values ( $\epsilon \approx 10^5 \text{ M}^{-1} \text{ cm}^{-1}$ ) in agreement with  $\pi-\pi^*$  transitions were observed. The fluorescence emission spectra for each dye were obtained using the relevant absorption maximum ( $\lambda_{\text{abs}}$ ) as the excitation wavelength. For all symmetrical cyanines one main emission band can be observed at around 667 nm, with a Stokes shift of 17 nm (399 cm<sup>-1</sup>). For all of the studied dyes, a small solvatochromic effect could be observed in the ground and excited states (~10 nm), which is probably due to solvent effects. The excitation spectra (Supporting Information) were also obtained and are quite similar to the UV–vis absorption spectra, a fact indicating that

**Table 1. Relevant Photophysical Data from UV–Vis Absorption and Fluorescence Emission of the Cyanine Dyes 1–9<sup>a</sup>**

dye	solvent	$\lambda_{\text{abs}}$	$\epsilon$	$\lambda_{\text{em}}$	$\Delta\lambda_{\text{ST}}$	$\Phi_{\text{f}}$
1	CHCl <sub>3</sub>	656	0.99	671	15/341	0.28
	EtOH	643	1.17	661	18/424	0.28
	DMF	644	0.94	662	18/422	0.42
	DMSO	647	1.35	665	18/418	0.39
	PBS	638	1.36	655	17/407	0.13
2	CHCl <sub>3</sub>	658	0.93	673	15/339	0.27
	EtOH	646	1.18	664	18/420	0.28
	DMF	648	1.03	665	17/395	0.39
	DMSO	650	1.38	667	17/392	0.43
	PBS	638	1.70	658	20/476	0.16
3	CHCl <sub>3</sub>	659	1.07	675	16/360	0.25
	EtOH	646	1.26	665	19/442	0.31
	DMF	648	1.36	666	18/417	0.41
	DMSO	650	1.18	668	18/415	0.41
	PBS	644	0.89	658	14/330	0.13
4	CHCl <sub>3</sub>	658	0.90	674	16/361	0.17
	EtOH	645	1.18	662	17/398	0.15
	DMF	646	1.12	664	18/420	0.20
	DMSO	648	1.34	666	18/417	0.22
	PBS	640	1.34	655	15/358	0.14
5	CHCl <sub>3</sub>	660	1.02	678	18/102	0.16
	EtOH	644	0.99	666	22/513	0.13
	DMF	648	1.58	669	21/484	0.14
	DMSO	650	0.85	674	24/548	0.15
	PBS	639	1.19	659	20/475	0.25
6	CHCl <sub>3</sub>	658	1.14	674	16/361	0.14
	EtOH	646	1.31	664	18/420	0.32
	DMF	648	1.30	665	17/395	0.40
	DMSO	650	1.31	666	16/370	0.41
	PBS	643	1.50	658	15/355	0.23
7	CHCl <sub>3</sub>	660	1.10	678	18/402	0.20
	EtOH	646	0.81	669	23/532	0.29
	DMF	650	0.98	670	20/459	0.32
	DMSO	654	0.89	675	21/476	0.29
	PBS	639	1.60	659	20/475	0.45
8	CHCl <sub>3</sub>	658	1.22	674	16/361	0.24
	EtOH	646	1.95	664	18/420	0.22
	DMF	648	1.24	665	17/395	0.38
	DMSO	651	1.34	668	17/391	0.45
	PBS	640	1.30	655	15/358	0.20
9	CHCl <sub>3</sub>	659	1.00	677	18/403	0.15
	EtOH	646	0.87	668	22/510	0.27
	DMF	650	0.99	670	20/459	0.31
	DMSO	653	1.45	675	22/499	0.30
	PBS	642	0.90	660	18/425	0.24

<sup>a</sup> $\lambda_{\text{abs}}$  and  $\lambda_{\text{em}}$  are the absorption and emission maxima in nanometers, respectively,  $\epsilon$  ( $\times 10^5 \text{ L mol}^{-1} \text{ cm}^{-1}$ ) is the molar extinction coefficient,  $\Phi_{\text{f}}$  is the quantum yield of fluorescence, and  $\Delta\lambda_{\text{ST}}$  is the Stokes shift ( $\text{nm}/\text{cm}^{-1}$ ).

no significant conformational or electronic changes took place in the excited state.

In Figure 4 are presented the UV–vis absorption and fluorescence emission spectra from carboxylated asymmetrical cyanines 4–9. An absorption band maximum located around 651 nm, with high molar extinction coefficient values ( $\epsilon \approx 10^5 \text{ M}^{-1} \text{ cm}^{-1}$ ) also in agreement with  $\pi$ – $\pi^*$  transitions could be observed. It can be seen that changes in the electronic structure

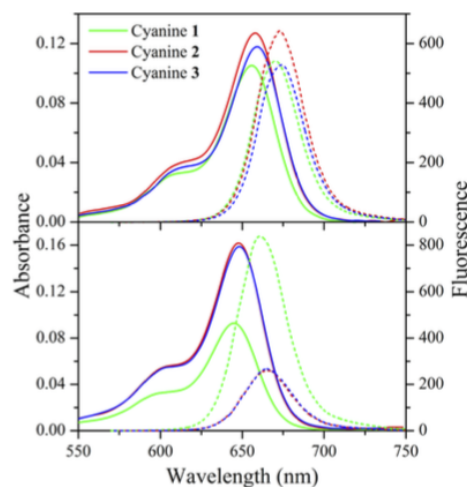


**Figure 3.** Absorption (solid line) and fluorescence emission (dashed line) spectra of the symmetrical cyanines 1–3 in CHCl<sub>3</sub> (top) and DMF (bottom). Conditions: dye concentration,  $\sim 10^{-6} \text{ M}$ ; cell path length, 1 cm.

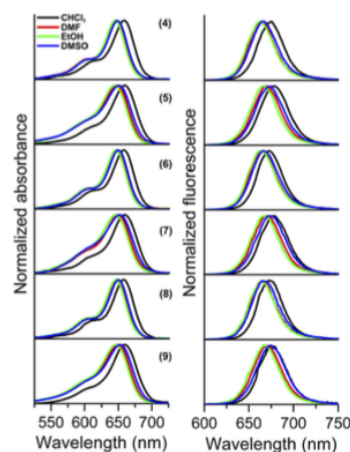


**Figure 4.** Absorption and fluorescence emission spectra in solution of the cyanines 4–9. Conditions: dye concentration,  $\sim 10^{-5} \text{ M}$ ; cell path length, 1 cm.

of these compounds (symmetrical to asymmetrical) did not play a fundamental role in the absorption spectra. Additionally, it can be observed that the cyanines 4–9 present one main fluorescence emission maximum located around 670 nm. The excitation spectra were also obtained and are quite similar to the UV–vis absorption spectra (Supporting Information). It is well-known that cyanines can present J- or H-type aggregates in solution.<sup>40–45</sup> These aggregates usually will present photophysical behavior different from those observed for the monomeric cyanines. J-type aggregates present red-shifted absorption, and H-type aggregates present blue-shifted bands. There are reports in the literature that the absorption bands shift around 50 nm from the absorption of the monomeric cyanines.<sup>40–43</sup> In this way, any evidence of aggregations in organic solution in the ground state could not be obtained for these dyes at the studied concentration. Additionally, the shape of the absorption UV–vis spectra in organic solvents is typical

of the molecular spectra of cyanine and other polymethine dyes. The band at longest wavelengths is the most intense band and represents approximately the  $0 \rightarrow 0$  transition in a vibronic progression. As pointed out by Pearce et al.<sup>43</sup> the pattern of subsidiary shoulders at shorter wavelengths differs from dye to dye in resolution and intensity and can be related to  $0 \rightarrow 1$ ,  $0 \rightarrow 2$ , etc. transitions of a dominant vibrational mode of frequency approximately  $1200 \text{ cm}^{-1}$ , which in our study was around  $1215 \text{ cm}^{-1}$ .

It is worth mentioning that the cyanines in PBS presented absorption and fluorescence emission spectra with shapes and maxima locations similar to those observed in organic solvents (Figure 5). Additionally, a study of the dependence of UV-vis

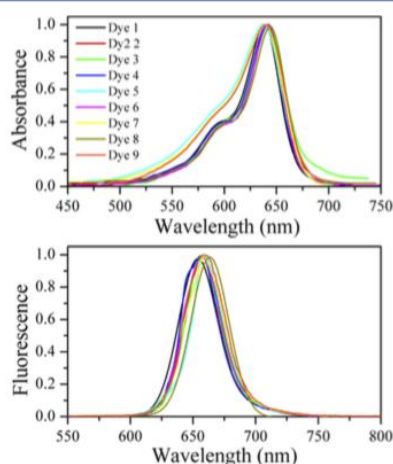


**Figure 5.** Normalized absorption and fluorescence emission spectra in PBS solution of the cyanines 1–9. Conditions: dye concentration,  $\sim 10^{-6} \text{ M}$ ; cell path length, 1 cm.

absorption in PBS on the dye concentration from  $10^{-3} \text{ M}$  up to  $10^{-7} \text{ M}$  was also performed (Supporting Information). The results indicate that any aggregation in the ground state could not be obtained in the solutions used in the BSA association study ( $10^{-6} \text{ M}$ ). Only at higher concentrations ( $10^{-3}$ – $10^{-4} \text{ M}$ ) did dyes 2, 4 and 9 present some evidence of J-type aggregates due to a red-shifted band around 750 nm.<sup>43</sup> Due to the lower solubility of the cyanines 8 and 9 in PBS, it was not possible to obtain good UV-vis spectra at concentrations higher than  $10^{-4} \text{ M}$ . The fluorescence emission spectra also showed very weak red-shifted emission curves at higher concentration, which could also be related to aggregates in solution.

**BSA Association.** The BSA association study was performed with different amounts of protein (0–12  $\mu\text{M}$  in PBS) added to a cyanine dye solution (2  $\mu\text{M}$  in PBS). Figure 6 depicts the UV-vis absorption spectra of cyanine dyes 5, 8, and 9 in the absence and presence of BSA. The additional curves from dyes 1–4 and 6 are presented in the Supporting Information and present a similar behavior. Evidences of J-type aggregates could be observed for cyanine 7 during the titration only in the presence of BSA due to the small red shift absorption located around 760 nm (Supporting Information).<sup>43</sup>

The spectra show two distinct sets of curves, which can be related to absorption regions from the protein (250–300 nm) and cyanine dye (500–700 nm). It can be observed that the increase of BSA raised the absorption intensity between 250

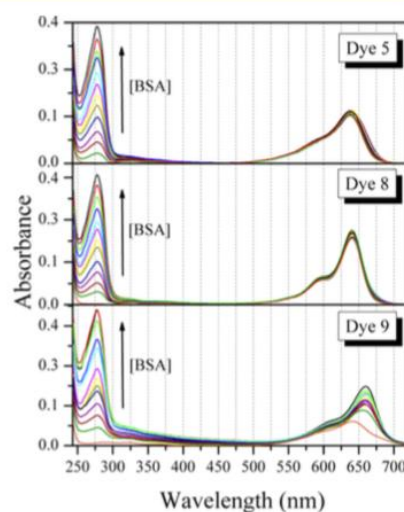


**Figure 6.** UV-vis spectra of the cyanine dyes 5, 8, and 9 at different BSA concentrations (0–12  $\mu\text{M}$ ). Conditions: dye concentration, 2  $\mu\text{M}$ ; cell path length, 1 cm.

and 300 nm, as expected. However, concerning the region from the cyanine dye, two distinct behaviors were observed. Independent of the BSA amount, dyes 5 and 8 showed an absorption located around 637 nm with nearly constant intensity. Despite the intense absorption in the absence of BSA, dye 9 increased in absorbance intensity after BSA addition, although there are reports in the literature that the addition of protein leads to an initial drop of the absorption maxima followed by a gradual increase of its intensity up to about the initial value.<sup>23</sup> Additionally, the BSA in solution red-shifts the absorption maxima by 25 nm, as already observed for similar structures.<sup>23</sup> The absorption maxima observed for dye 9 in the presence of BSA can probably be related to the conjugate BSA–cyanine dye in the ground state. The slight changes in the UV-vis absorption intensity and maxima location for dyes 5 and 8 in the presence of BSA do not discard at all the presence of conjugates in solution. Since there are no isosbestic points in the absorption spectra of the dye 9 in the presence of the BSA, it can be supposed that the equilibrium between the free and the bound dye is not simple.<sup>23</sup>

Bovine serum albumin (BSA) is a globular protein composed of three structurally similar domains, each containing 2 subdomains (A and B) stabilized by 17 disulfide bridges.<sup>46–50</sup> It is well-known that aromatic and heterocyclic ligands were found to bind within two hydrophobic sites in subdomains IIA and IIIA, namely site I and site II.<sup>46–51</sup> In serum albumin, it was suggested that cyanine dyes exhibit a high specificity for the subdomain IIIA (site II).<sup>52–55</sup> Although it was already presented in the literature that the binding affinity of some cyanines of these dyes not only is hydrophobicity dependent but may be influenced by steric interferences within the binding sites,<sup>55</sup> there is a general outline that increased hydrophobicity among the dyes increases binding affinity with the protein. In this way, comparing the UV-vis data on the series of the studied cyanine dyes, we can suppose that not only do the alkyl chains drive the affinity of the dye to the protein in the ground state<sup>56,57</sup> but also steric hindrance due to additional moieties present in the dye can play an important role. In addition, it is



worth mentioning that the same behavior was observed for all synthesized dyes with similar chemical structures.

Characteristics of fluorescence emission spectra of the dyes 5, 8, and 9 in the absence and presence of BSA are given in Figure 7. The additional curves from dyes 1–4, 6, and 7 are presented in the Supporting Information.

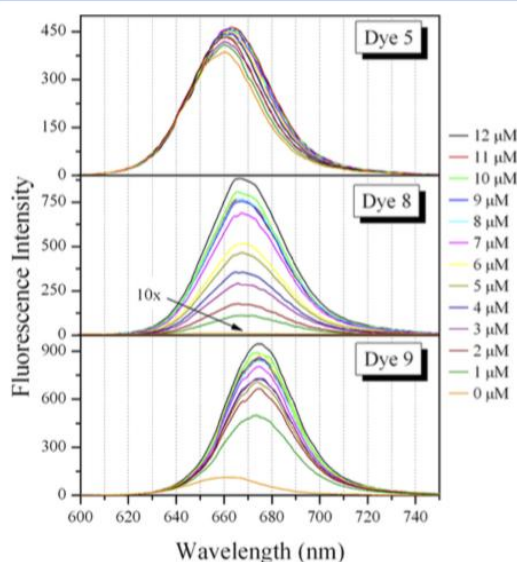


**Figure 7.** Fluorescence emission spectra of the cyanine dyes 5, 8, and 9 at different BSA concentrations (0–12  $\mu\text{M}$ ). The curve from dye 8 in the absence of BSA was magnified 10 times in order to be observed in this figure. Conditions: dye concentration, 2  $\mu\text{M}$ ; cell path length, 1 cm.

It should be noted that, despite the reported dyes in the literature, these compounds do not present new fluorescence emission bands due to aggregates in solution,<sup>26,44,45</sup> since usually optical sensors to detect proteins in solution present nonfluorescent aggregates, which in the presence of the protein increase the fluorescence emission of the bound dye due to disruption of these nonfluorescent aggregates. However, the cyanine dyes reported in this work behave differently. Dye 5 presented a significant fluorescence emission in PBS located at the same region observed in organic solvents, as well as linearity for the Lambert–Beer plot observed in the UV–vis spectra, indicating that dye 5 does not aggregate in PBS. Additionally, we could not observe a linear correlation between the fluorescence intensity and protein concentration. The same results were observed for dyes 1, 2, 4, and 6 (Figure 8). On the other hand, dyes 3 and 7–9 presented fluorescence intensity which increased with the BSA amount in solution. Dyes 3, 7, and 9 presented fluorescence in the absence of albumin. The first addition of BSA (1  $\mu\text{M}$ ) increased the fluorescence emission 2–4 times. After the last addition of protein (12  $\mu\text{M}$ ) the fluorescence increased 4–8 times, depending on the cyanine dye, and the emission maxima red-shifts around 20 nm. The observed bathochromic shift suggests that the BSA microenvironments are less polar than that of PBS due to the hydrophobic groups present in the surface and interiors of the BSA.<sup>58</sup> Moreover, dye 8 was nearly nonfluorescent in the absence of BSA and the fluorescence intensity increased 50 and

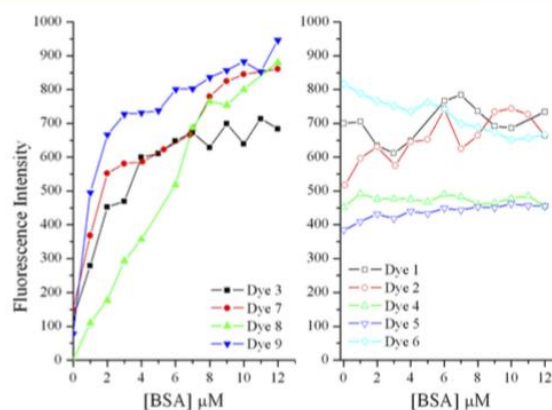


**Figure 8.** Plot of fluorescence intensity maxima of the cyanine dyes 1–9 as a function of BSA concentration. Conditions: pH 7.0; room temperature.

450 times after addition of 1 and 12  $\mu\text{M}$  of BSA, respectively. This result probably indicates that dye 8 presented a higher affinity with the protein due to a higher hydrophobic character, allowed by combination of the long alkyl chain as well as the methyl groups present in the indoleninium ring. Since the fluorescence intensity increase with the BSA content was nonlinear for some cyanine dyes, it was possible to observe two sets of compounds. The first set was dyes 1, 2, 4, and 6, where the variation is almost constant. The second set was dyes 3 and 7–9, where a linear increase of the fluorescence intensity could be obtained, as follows: dye 3 (0–2  $\mu\text{M}$ ;  $\Delta c = 2 \mu\text{M}$ ;  $R^2 = 0.997$ ); dye 7 (0–2  $\mu\text{M}$ ;  $\Delta c = 2 \mu\text{M}$ ;  $R^2 = 0.995$ ); dye 8 (0–8  $\mu\text{M}$ ;  $\Delta c = 8 \mu\text{M}$ ;  $R^2 = 0.990$ ) and dye 9 (0–2  $\mu\text{M}$ ;  $\Delta c = 2 \mu\text{M}$ ;  $R^2 = 0.900$ ).

Since it could be observed that these compounds interact differently with the protein, and the ability to bind dyes depends on the protein concentration,<sup>59</sup> a plot of the relative fluorescence intensity ( $F/F_0$ ) of the cyanine dyes 1–9 against the ratio of the dye concentration to the concentration of BSA ( $C/P$ ) in PBS was made (Figure 9).

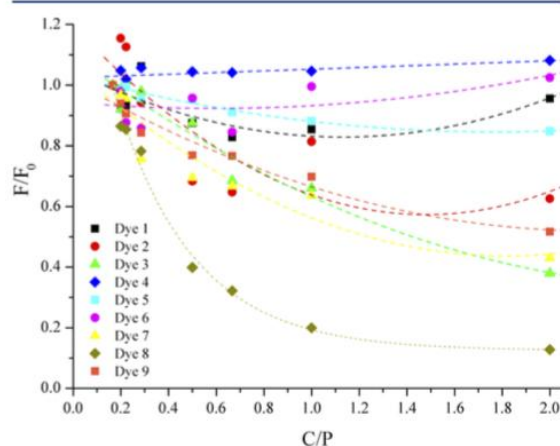


**Figure 9.** Fluorescence intensity of cyanine dyes 1–9 relative to the concentration of BSA in PBS at room temperature.

As discussed by Kurtaliev et al.,<sup>59</sup> in this plot, the fall of the fluorescence intensity of the interaction of BSA with dyes cannot be related only to the formation of nonfluorescent complexes but is also due to a change in the conformation of albumin. For the successful application of dyes as a probe, it is necessary to bind to the protein with no damage to its structure. At the point where the probe is located, conformational changes in the protein inevitably occur. The higher the concentration of the dye, the more damaging its activity. Therefore, at higher degrees of binding dyes can significantly change the conformation of albumin. Hence it is important to select the optimal concentration of dye and protein. Promising results were obtained for cyanines 2, 3, 5, and 7–9. For these compounds the binding constants were obtained (Figure 10) with values similar to those reported in the literature to parent cyanine dyes ((1.19–9.49) × 10<sup>5</sup> M<sup>-1</sup>) (Supporting Information).<sup>59–61</sup>

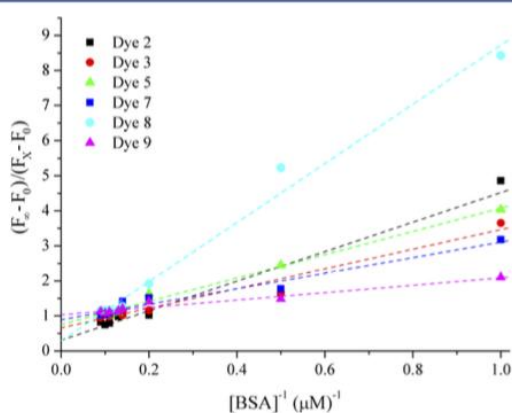


Figure 10. Plot of  $(F_{\infty} - F_0)/(F_x - F_0)$  against  $[BSA]^{-1}$ , where [dye] =  $2.0 \times 10^{-5}$  M.

## CONCLUSION

A series of symmetrical and asymmetrical cyanines was efficiently obtained from quaternary heterocyclic ammonium salts containing *N*-alkyl (ethyl, butyl, and octyl) and *N*-carboxypentyl groups. The cyanine dyes were prepared through activated intermediates by a practical synthetic route in satisfactory overall yield from commercially available and relatively inexpensive starting materials. It could be observed that the fluorescence intensity of the cyanine dyes containing longer alkyl chains was enhanced noticeably in the presence of protein. However, the intricate photophysical behavior of these dyes in the presence of protein indicated that the combination of the alkyl chain length present in the quaternized nitrogen and the electronic and steric characteristics of the indoleninium ring tailored the optical sensing application of the studied compounds. Additionally, the binding constants could be obtained and the values are in agreement with previously reported data for parent cyanines.

## EXPERIMENTAL SECTION

**Materials and Methods.** <sup>1</sup>H and <sup>13</sup>C NMR data were determined in CDCl<sub>3</sub>, DMSO-*d*<sub>6</sub>, or CD<sub>3</sub>OD-*d*<sub>4</sub> solutions on an NMR spectrometer operating at 299.98 MHz for <sup>1</sup>H and at 75.42 MHz for <sup>13</sup>C. The chemical shifts are expressed as  $\delta$  (ppm) relative to

tetramethylsilane as an internal standard. Splitting patterns are designed as follows; s, singlet; d, doublet; t, triplet; q, quartet; m, multiplet; br s, broad singlet. All of the detected signals were in accordance with the proposed structures. FTIR spectra were recorded on an IR spectrophotometer. High-resolution mass spectra were recorded with electrospray ionization (HRMS-ESI) data in the positive mode using a Micromass Q-ToF instrument. Samples were infused by a 100  $\mu$ L syringe at a flow rate ranging from 5 to 10  $\mu$ L min<sup>-1</sup> depending on the sample. The following typical operating conditions were used: 3 kV capillary voltage, 33 V sample cone voltage, 2.5 V extraction cone voltage, and desolvation gas temperature of 100 °C. N<sub>2</sub> was used as the desolvation gas, and methanol was the solvent used with all samples. Purification by column chromatography was carried out on silica gel 60 (70–230 mesh). Analytical thin-layer chromatography (TLC) was conducted on aluminum plates with 0.2 mm of silica gel 60F-254. 2,3,3-Trimethylindolenine (10), bromoethane, 1-iodobutane, 1-iodooctane, 6-bromohexanoic acid, and 1,1,3,3-tetramethoxypropane (17) were used without purification. 2-Methylbenzothiazole (14) was prepared according to a methodology previously described.<sup>62</sup> The UV-vis absorption spectra were measured on an UV spectrophotometer. The steady-state fluorescence emission spectra were obtained on a spectrofluorophotometer with subsequent correction for the instrument spectral sensitivity. Spectroscopic grade solvents were used in UV-vis absorption and fluorescence emission measurements. The quantum yields of fluorescence ( $\Phi_f$ ) were obtained at 25 °C in spectroscopic grade solvents using the optical dilute method: absorbance lower than 0.05. For the calculation of quantum yields of fluorescence, the refraction indexes of solvents were taken into account. Zinc phthalocyanine (ZnPc) was synthesized and purified according to the literature<sup>63</sup> and used as a quantum yield standard ( $\Phi_f = 0.20$  in DMSO).<sup>64</sup> The quantum yields of fluorescence in PBS were measured using an optimal wavelength for excitation such that the sample and the standard were excited at an almost plateau-like region of their absorption spectra.<sup>65</sup> Bovine serum albumin (BSA) fraction V was used in the BSA experiments.

**Quaternary Heterocyclic Ammonium Salt Precursors. *N*-Ethyl-2,3,3-trimethylindoleninium Bromide (11).** A mixture of bromoethane (0.68 g, 6.28 mmol) and 2,3,3-trimethylindolenine (10; 0.5 g, 3.14 mmol) in *o*-dichlorobenzene (3 mL) was heated to 120 °C for 24 h. After it was cooled to room temperature, the resulting mixture was filtered and the residue was washed successively with hexane (3 × 5 mL) and Et<sub>2</sub>O (3 × 5 mL). The solid was dried under vacuum to give 0.42 g (2.23 mmol, 70% yield) of *N*-ethyl-2,3,3-trimethylindoleninium bromide (11) as a red powder. <sup>1</sup>H NMR (300 MHz, CDCl<sub>3</sub>):  $\delta$  (ppm) 7.69–7.61 (m, 1H), 7.52–7.40 (m, 3H), 4.64 (q, 2H, *J* = 7.2 Hz), 3.01 (s, 3H), 1.50 (s, 6H), 1.49 (t, 3H, *J* = 7.2 Hz). <sup>13</sup>C NMR (75 MHz, CDCl<sub>3</sub>):  $\delta$  (ppm) 195.6, 141.5, 140.4, 129.9, 129.4, 123.3, 115.2, 54.5, 44.7, 22.8, 15.9, 13.3.

***N*-Butyl-2,3,3-trimethylindoleninium Iodide (12).** A mixture of 1-iodobutane (1.2 g, 6.52 mmol) and 2,3,3-trimethylindolenine (10; 0.21 g, 1.30 mmol) was heated to 145 °C for 3 h. After it was cooled, the resulting mixture was purified by column chromatography using silica gel and CH<sub>2</sub>Cl<sub>2</sub>/MeOH (90/10) as the eluent mixture to give 0.23 g (1.07 mmol, 82% yield) of 12 as a red powder. <sup>1</sup>H NMR (300 MHz, CDCl<sub>3</sub>):  $\delta$  (ppm) 7.80–7.69 (m, 1H), 7.68–7.52 (m, 3H), 4.67 (t, 2H, *J* = 7.2 Hz), 3.13 (s, 3H), 2.04–1.88 (m, 2H), 1.67 (s, 6H), 1.60–1.44 (m, 2H), 1.01 (t, 3H, *J* = 7.2 Hz). <sup>13</sup>C NMR (75 MHz, CDCl<sub>3</sub>):  $\delta$  (ppm) 195.6, 141.5, 140.8, 130.1, 129.4, 123.4, 115.3, 54.6, 49.7, 29.9, 23.1, 20.1, 17.0, 13.6.

***N*-Octyl-2,3,3-trimethylindoleninium Iodide (13).** A mixture of 1-iodooctane (1.2 g, 5.0 mmol) and 2,3,3-trimethylindolenine (10; 0.16 g, 1.0 mmol) was heated to 145 °C for 3 h. After it was cooled, the resulting mixture was purified by column chromatography using silica gel and CH<sub>2</sub>Cl<sub>2</sub>/MeOH (80/20) as the eluent mixture to give 0.2 g (0.75 mmol, 75% yield) of 13. <sup>1</sup>H NMR (300 MHz, CDCl<sub>3</sub>):  $\delta$  (ppm) 7.69–7.58 (m, 1H), 7.57–7.50 (m, 3H), 4.60 (t, 2H, *J* = 7.8 Hz), 3.05 (s, 3H), 1.95–1.85 (m, 2H), 1.62 (s, 6H), 1.48–1.32 (m, 2H), 1.32–1.17 (m, 8H), 0.82 (t, 3H, *J* = 6.6 Hz). <sup>13</sup>C NMR (75 MHz, CDCl<sub>3</sub>):  $\delta$  (ppm) 195.4, 141.5, 140.7, 130.2, 129.5, 123.5, 115.3, 54.7, 49.9, 31.5, 28.9, 28.8, 28.0, 26.7, 23.1, 22.5, 16.8, 14.0.

**1-(5-Carboxypentyl)-2,3,3-trimethylindoleninium Bromide (15).** A mixture of 6-bromohexanoic acid (2.7 g, 13.5 mmol) and 2,3,3-trimethylindolenine (10; 1.5 g, 9.37 mmol) in *o*-dichlorobenzene (10 mL) was heated to 120 °C for 24 h. After it was cooled to room temperature, the mixture was filtered and the residue was washed successively with hexane (3 × 5 mL) and Et<sub>2</sub>O (3 × 5 mL). The resulting solid was purified by column chromatography using silica gel and CH<sub>2</sub>Cl<sub>2</sub>/MeOH (80/20) as the eluent mixture to give 1.67 g (6.08 mmol, 65% yield) of 15. <sup>1</sup>H NMR (300 MHz, DMSO-*d*<sub>6</sub>): δ (ppm) 12.05 (br s, 1H), 8.05–7.98 (m, 1H), 7.88–7.85 (m, 1H), 7.64–7.55 (m, 2H), 4.49 (t, 2H, *J* = 7.2 Hz), 2.89 (s, 3H), 2.22 (t, 2H, *J* = 7.2 Hz), 1.95–1.75 (m, 2H), 1.57 (m, 2H), 1.55 (s, 6H), 1.54–1.35 (m, 2H). <sup>13</sup>C NMR (75 MHz, DMSO-*d*<sub>6</sub>): δ (ppm) 196.5, 174.3, 141.9, 141.1, 129.4, 128.9, 123.6, 115.6, 54.2, 47.5, 33.4, 27.0, 25.4, 24.1, 22.0, 14.3.

**3-(5-Carboxypentyl)-2-methylbenzo[d]thiazol-3-ium Bromide (16).** A mixture of 6-bromohexanoic acid (1.0 g, 6.71 mmol) and 2-methylbenzothiazole (14; 1.88 g, 9.67 mmol) in *o*-dichlorobenzene (10 mL) was heated to 120 °C for 7 days. After it was cooled to room temperature, the resulting mixture was filtered and the residue was washed successively with hexane (3 × 5 mL) and Et<sub>2</sub>O (3 × 5 mL). The solid was dried under vacuum to give 0.71 g (2.68 mmol, 40% yield) of 16 as a gray powder. <sup>1</sup>H NMR (300 MHz, DMSO-*d*<sub>6</sub>): δ (ppm) 8.53 (d, 1H, *J* = 8.1 Hz), 8.37 (d, 1H, *J* = 8.1 Hz), 7.90 (t, 1H, *J* = 8.1 Hz), 7.81 (t, 1H, *J* = 8.1 Hz), 4.74 (t, 2H, *J* = 7.5 Hz), 3.25 (s, 3H), 2.24 (t, 2H, *J* = 6.9 Hz), 1.87 (m, 2H), 1.64–1.40 (m, 4H). <sup>13</sup>C NMR (75 MHz, DMSO-*d*<sub>6</sub>): δ (ppm) 177.1, 174.4, 140.8, 129.4, 129.1, 128.1, 124.7, 116.9, 49.1, 33.5, 27.5, 25.4, 24.0, 17.0.

**General Procedure for Symmetrical Cyanine Dye Synthesis.** A mixture of malondialdehyde dianil hydrochloride (18; 1.2 equiv) and the quaternary heterocyclic ammonium salt (1.0 equiv) in acetic anhydride was refluxed for 2 h. The solution was cooled to room temperature, and the solvent was removed by distilling. Next, a mixture of the crude product containing mainly the enamide, quaternary heterocyclic ammonium salt (1.0 equiv), and anhydrous sodium acetate (2.1 equiv), in absolute ethanol and under an inert atmosphere, was refluxed over 6 h. The solution was cooled to room temperature, and the solvent was removed under reduced pressure.

***N*-((1*E*)-3-(Phenylimino)prop-1-enyl)benzenamine Hydrochloride (18).** A solution of distilled water (70 mL), concentrated HCl (5 mL), and aniline (3.7 mL, 40 mmol) was added dropwise to a solution of water (85 mL), concentrated HCl (4.3 mL), and 1,1,3,3-tetramethoxypropane (17; 5.3 mL, 30 mmol) with stirring at 50 °C. After 2 h, the precipitate was isolated by filtration to give 6.2 g (85% yield) of 18 as a, orange solid. <sup>1</sup>H NMR (300 MHz, DMSO-*d*<sub>6</sub>): δ (ppm) 12.75 (d, 2H, *J* = 13.5 Hz), 8.97 (t, 2H, *J* = 12.6 Hz), 7.46 (m, 8H), 7.32–7.18 (m, 2H), 6.55 (t, 1H, *J* = 11.4 Hz). <sup>13</sup>C NMR (75 MHz, DMSO-*d*<sub>6</sub>): δ (ppm) 158.4, 138.7, 129.9, 129.5, 117.4, 98.7.

**Cyanine Dye 1.** The resulting solid was purified by column chromatography using silica gel and CH<sub>2</sub>Cl<sub>2</sub>/MeOH (90/10) as the eluent mixture. Yield: 58%. FTIR (KBr, cm<sup>-1</sup>): ν 2968, 1494, 1454, 1378, 1331, 1169, 1105, 1071. <sup>1</sup>H NMR (300 MHz, CDCl<sub>3</sub>): δ (ppm) 8.25 (t, 2H, *J* = 12.9 Hz), 7.46–7.32 (m, 4H), 7.22 (t, 2H, *J* = 7.5 Hz), 7.14 (d, 2H, *J* = 8.4 Hz), 6.77 (t, 1H, *J* = 12.3 Hz), 6.32 (d, 2H, *J* = 13.5 Hz), 4.17 (q, 4H, *J* = 7.5 Hz), 1.79 (s, 12H), 1.44 (t, 6H, *J* = 6.9 Hz). <sup>13</sup>C NMR (75 MHz, CDCl<sub>3</sub>): δ (ppm) 172.6, 154.0, 141.6, 141.4, 128.5, 126.1, 125.0, 122.3, 110.3, 103.3, 49.9, 39.4, 28.0, 12.4. HRMS (ESI-qTOF): *m/z* [M + H]<sup>+</sup> calcd for C<sub>29</sub>H<sub>35</sub>N<sub>2</sub> 412.2878, found 412.2897.

**Cyanine Dye 2.** The resulting solid was purified by column chromatography using silica gel and CH<sub>2</sub>Cl<sub>2</sub>/MeOH (80/20) as the eluent mixture. Yield: 55%. FTIR (KBr, cm<sup>-1</sup>): ν 2956, 1493, 1454, 1384, 1334, 1219, 1167, 1095. <sup>1</sup>H NMR (300 MHz, CDCl<sub>3</sub>): δ (ppm) 8.34 (t, 2H, *J* = 13.2 Hz), 7.44–7.30 (m, 4H), 7.21 (t, 2H, *J* = 6.9 Hz), 7.09 (d, 2H, *J* = 7.8 Hz), 6.74 (t, 1H, *J* = 12.6 Hz), 6.28 (d, 2H, *J* = 13.8 Hz), 4.07 (t, 4H, *J* = 7.5 Hz), 1.86–1.74 (m, 4H), 1.81 (s, 12H), 1.49 (m, 4H), 1.00 (t, 6H, *J* = 7.2 Hz). <sup>13</sup>C NMR (75 MHz, CDCl<sub>3</sub>): δ (ppm) 173.3, 154.3, 142.2, 141.6, 128.5, 126.2, 125.1, 122.4, 110.5, 103.6, 49.6, 44.3, 29.6, 28.1, 20.4, 14.0. HRMS (ESI-qTOF): *m/z* [M + H]<sup>+</sup> calcd for C<sub>33</sub>H<sub>43</sub>N<sub>2</sub> 468.3504, found 468.3523.

**Cyanine Dye 3.** The resulting solid was purified by column chromatography using silica gel and CH<sub>2</sub>Cl<sub>2</sub>/MeOH (80/20) as the eluent mixture. Yield: 50%. FTIR (KBr, cm<sup>-1</sup>): ν 2924, 1491, 1453, 1383, 1334, 1141, 1099, 1015. <sup>1</sup>H NMR (300 MHz, CDCl<sub>3</sub>): δ (ppm) 8.18 (t, 2H, *J* = 12.9 Hz), 7.38–7.28 (m, 4H), 7.18 (t, 2H, *J* = 7.5 Hz), 7.05 (d, 2H, *J* = 7.8 Hz), 6.70 (t, 1H, *J* = 12.3 Hz), 6.21 (d, 2H, *J* = 13.5 Hz), 4.02 (t, 4H, *J* = 7.5 Hz), 1.85–1.65 (m, 2H), 1.76 (s, 12H), 1.48–1.30 (m, 2H), 1.40–1.21 (m, 20H), 0.82 (t, 6H, *J* = 6.6 Hz). <sup>13</sup>C NMR (75 MHz, CDCl<sub>3</sub>): δ (ppm) 173.1, 153.8, 142.1, 141.5, 128.6, 126.0, 125.2, 122.4, 110.6, 103.6, 49.6, 44.6, 31.8, 29.4, 29.1, 28.2, 27.5, 27.0, 22.6, 14.2. HRMS (ESI-qTOF): *m/z* [M + H]<sup>+</sup> calcd for C<sub>41</sub>H<sub>59</sub>N<sub>2</sub> 580.4756, found 580.4758.

**General Procedure for Asymmetrical Cyanine Dye Synthesis.** A mixture of malondialdehyde dianil hydrochloride (18; 1.2 equiv) and the quaternary heterocyclic ammonium salt (1.0 equiv) in acetic anhydride was refluxed for 2 h. The solution was cooled to room temperature, and the solvent was removed by distilling. Next, a mixture of the crude product containing mainly the enamide, quaternary heterocyclic ammonium salt (1.0 equiv), and anhydrous sodium acetate (2.1 equiv), in absolute ethanol and under an inert atmosphere, was refluxed over 3 h. The solution was cooled to room temperature, and the solvent was removed under reduced pressure.

**Cyanine Dye 4.** The resulting solid was purified by column chromatography using silica gel and CH<sub>2</sub>Cl<sub>2</sub>/MeOH (80/20) as the eluent mixture. Yield: 43%. FTIR (KBr, cm<sup>-1</sup>): ν 3407, 2925, 1720, 1493, 1454, 1378, 1332, 1149, 1109, 1074. <sup>1</sup>H NMR (300 MHz, CD<sub>3</sub>OD-*d*<sub>4</sub>): δ (ppm) 8.27 (t, 2H, *J* = 12.6 Hz), 7.58–7.46 (m, 2H), 7.45–7.36 (m, 2H), 7.35–7.18 (m, 4H), 6.66 (t, 1H, *J* = 12.6 Hz), 6.31 (dd, 2H, *J* = 13.2 Hz), 4.25–4.05 (m, 4H), 2.32 (t, 2H, *J* = 7.2 Hz), 1.90–1.75 (m, 2H), 1.72 (s, 12H), 1.74–1.62 (m, 2H), 1.58–1.42 (m, 2H), 1.39 (t, 3H, *J* = 7.2 Hz). <sup>13</sup>C NMR (75 MHz, CD<sub>3</sub>OD-*d*<sub>4</sub>): δ (ppm) 177.5, 174.6, 174.3, 155.6, 155.5, 143.5, 143.0, 142.8, 142.6, 129.8, 129.7, 126.7, 126.3, 126.2, 123.5, 123.4, 112.0, 111.8, 104.3, 104.1, 50.6, 50.5, 44.8, 40.0, 34.8, 28.1, 27.9 (2C), 27.8 (2C), 27.3, 25.7, 12.6. HRMS (ESI-qTOF): *m/z* [M + H]<sup>+</sup> calcd for C<sub>33</sub>H<sub>41</sub>N<sub>2</sub>O<sub>2</sub> 498.3246, found 498.3225.

**Cyanine Dye 5.** The resulting solid was purified by column chromatography using silica gel and CH<sub>2</sub>Cl<sub>2</sub>/MeOH (50/50) as the eluent mixture. Yield: 48%. FTIR (KBr, cm<sup>-1</sup>): ν 3409, 2923, 1718, 1502, 1456, 1440, 1381, 1151, 1108, 1074. <sup>1</sup>H NMR (300 MHz, CD<sub>3</sub>OD-*d*<sub>4</sub>): δ (ppm) 8.06–7.86 (m, 3H), 7.74 (d, 1H, *J* = 8.1 Hz), 7.61 (t, 1H, *J* = 8.1 Hz), 7.52–7.38 (m, 2H), 7.33 (t, 1H, *J* = 8.1 Hz), 7.22–7.08 (m, 2H), 6.64 (d, 1H, *J* = 13.2 Hz), 6.58 (t, 1H, *J* = 12.6 Hz), 6.08 (d, 1H, *J* = 13.2 Hz), 4.46 (t, 2H, *J* = 7.8 Hz), 4.03 (q, 2H, *J* = 7.5 Hz), 2.32 (t, 2H, *J* = 7.5 Hz), 1.95–1.80 (m, 2H), 1.78–1.60 (m, 2H), 1.67 (s, 6H), 1.62–1.43 (m, 2H), 1.33 (t, 3H, *J* = 7.2 Hz). <sup>13</sup>C NMR (75 MHz, CD<sub>3</sub>OD-*d*<sub>4</sub>): δ (ppm) 177.6, 171.0, 168.4, 154.0, 152.3, 143.5, 142.7, 142.0, 129.6, 129.5, 127.6, 127.2, 125.0, 124.4, 124.0, 123.2, 115.1, 110.7, 104.3, 101.5, 49.7, 48.0, 39.3, 34.9, 28.8, 28.1 (2C), 27.1, 25.7, 12.3. HRMS (ESI-qTOF): *m/z* [M + H]<sup>+</sup> calcd for C<sub>30</sub>H<sub>35</sub>N<sub>2</sub>O<sub>2</sub> 488.2498, found 488.2514.

**Cyanine Dye 6.** The resulting solid was purified by column chromatography using silica gel and CH<sub>2</sub>Cl<sub>2</sub>/MeOH (50/50) as the eluent mixture. Yield: 45%. FTIR (KBr, cm<sup>-1</sup>): ν 3420, 1492, 1453, 1383, 1334, 1147, 1093, 1016. <sup>1</sup>H NMR (300 MHz, DMSO-*d*<sub>6</sub>): δ (ppm) 8.37 (t, 2H, *J* = 13.2 Hz), 7.64 (d, 2H, *J* = 7.2 Hz), 7.46–7.36 (m, 4H), 7.30–7.20 (m, 2H), 6.62 (t, 1H, *J* = 12.3 Hz), 6.33 (d, 2H, *J* = 12.3 Hz), 4.11 (t, 4H, *J* = 7.5 Hz), 3.45 (br s, 1H), 2.20 (t, 2H, *J* = 6.6 Hz), 1.69 (s, 14H), 1.65–1.50 (m, 4H), 1.49–1.32 (m, 4H), 0.94 (t, 3H, *J* = 7.5 Hz). <sup>13</sup>C NMR (75 MHz, DMSO-*d*<sub>6</sub>): δ (ppm) 174.5, 172.6, 172.5, 154.1, 142.0, 141.1, 128.4, 125.6, 124.7, 122.5, 111.1, 103.2, 48.9, 43.3, 33.6, 29.1, 27.2, 26.7, 25.7, 24.3, 19.5, 13.8. HRMS (ESI-qTOF): *m/z* [M + H]<sup>+</sup> calcd for C<sub>35</sub>H<sub>45</sub>N<sub>2</sub>O<sub>2</sub> 526.3559, found 526.3547.

**Cyanine Dye 7.** The resulting solid was purified by column chromatography using silica gel and CH<sub>2</sub>Cl<sub>2</sub>/MeOH (50/50) as the eluent mixture. Yield: 40%. FTIR (KBr, cm<sup>-1</sup>): ν 3432, 2927, 1501, 1478, 1455, 1382, 1322, 1152, 1102. <sup>1</sup>H NMR (300 MHz, CD<sub>3</sub>OD-*d*<sub>4</sub>): δ (ppm) 7.99 (t, 1H, *J* = 12.9 Hz), 7.97 (t, 1H, *J* = 12.6 Hz), 7.88 (d, 1H, *J* = 7.8 Hz), 7.71 (d, 1H, *J* = 8.4 Hz), 7.55 (t, 1H, *J* = 7.5 Hz),

7.39 (t, 2H,  $J = 7.8$  Hz), 7.30 (t, 1H,  $J = 7.2$  Hz), 7.16–7.07 (m, 2H), 6.72–6.58 (m, 2H), 6.06 (d, 1H,  $J = 13.2$  Hz), 4.42 (t, 2H,  $J = 7.5$  Hz), 3.96 (t, 2H,  $J = 7.5$  Hz), 2.31 (t, 2H,  $J = 7.2$  Hz), 1.92–1.78 (m, 2H), 1.76–1.62 (m, 4H), 1.66 (s, 6H), 1.60–1.38 (m, 4H), 0.98 (t, 3H,  $J = 7.2$  Hz).  $^{13}\text{C}$  NMR (75 MHz,  $\text{CD}_3\text{OD}-d_4$ ):  $\delta$  (ppm) 177.5, 171.3, 168.2, 154.0, 152.1, 144.0, 142.6, 141.9, 129.6, 129.5, 127.6, 127.1, 124.9, 124.6, 124.1, 123.2, 115.1, 110.9, 104.4, 102.0, 49.6, 48.1, 44.3, 34.8, 30.3, 28.9, 28.4 (2C), 27.1, 25.7, 21.2, 14.4. HRMS (ESI-qTOF):  $m/z$   $[\text{M} + \text{H}]^+$  calcd for  $\text{C}_{32}\text{H}_{39}\text{N}_2\text{O}_2\text{S}$  516.2811, found 516.2816.

**Cyanine Dye 8.** The resulting solid was purified by column chromatography using silica gel and  $\text{CH}_2\text{Cl}_2/\text{MeOH}$  (50/50) as the eluent mixture. Yield: 46%. FTIR (KBr,  $\text{cm}^{-1}$ ):  $\nu$  3439, 1492, 1453, 1382, 1334, 1153, 1102, 1014.  $^1\text{H}$  NMR (300 MHz,  $\text{CD}_3\text{OD}-d_4$ ):  $\delta$  (ppm) 8.28 (t, 2H,  $J = 12.9$  Hz), 7.47 (d, 2H,  $J = 7.5$  Hz), 7.39 (t, 2H,  $J = 7.5$  Hz), 7.34–7.18 (m, 4H), 6.74 (t, 1H,  $J = 12.6$  Hz), 6.34 (d, 2H,  $J = 13.8$  Hz), 4.12 (t, 4H,  $J = 6.9$  Hz), 2.31 (t, 2H,  $J = 6.9$  Hz), 1.89–1.70 (m, 4H), 1.72 (s, 12H), 1.80–1.60 (m, 2H), 1.58–1.40 (m, 4H), 1.45–1.25 (m, 8H), 0.87 (t, 3H,  $J = 6.9$  Hz).  $^{13}\text{C}$  NMR (75 MHz,  $\text{CD}_3\text{OD}-d_4$ ):  $\delta$  (ppm) 177.2, 174.6, 174.5, 155.3, 143.5, 142.7, 142.6, 129.7, 126.9, 126.2, 162.1, 123.4, 112.1, 112.0, 104.6, 104.4, 50.6, 50.5, 45.0, 44.8, 34.7, 32.8, 30.4, 30.2, 28.5, 28.2, 28.1, 27.8, 27.3, 25.7, 23.7, 14.5. HRMS (ESI-qTOF):  $m/z$   $[\text{M} + \text{H}]^+$  calcd for  $\text{C}_{39}\text{H}_{33}\text{N}_2\text{O}_2$  582.4185, found 582.4188.

**Cyanine Dye 9.** The resulting solid was purified by column chromatography using silica gel and  $\text{CH}_2\text{Cl}_2/\text{MeOH}$  (50/50) as the eluent mixture. Yield: 50%. FTIR (KBr,  $\text{cm}^{-1}$ ):  $\nu$  3437, 2924, 1502, 1477, 1455, 1383, 1322, 1148, 1108.  $^1\text{H}$  NMR (300 MHz,  $\text{CD}_3\text{OD}-d_4$ ):  $\delta$  (ppm) 8.00 (t, 1H,  $J = 12.9$  Hz), 7.97 (t, 1H,  $J = 12.6$  Hz), 7.89 (d, 1H,  $J = 7.8$  Hz), 7.71 (d, 1H,  $J = 8.1$  Hz), 7.56 (t, 1H,  $J = 7.2$  Hz), 7.46–7.36 (m, 2H), 7.31 (t, 1H,  $J = 7.8$  Hz), 7.18–7.04 (m, 2H), 6.66 (d, 1H,  $J = 13.8$  Hz), 6.63 (t, 1H,  $J = 12.6$  Hz), 6.06 (d, 1H,  $J = 13.2$  Hz), 4.43 (t, 2H,  $J = 7.5$  Hz), 3.96 (t, 2H,  $J = 7.5$  Hz), 2.31 (t, 2H,  $J = 6.9$  Hz), 1.92–1.70 (m, 2H), 1.80–1.60 (m, 4H), 1.67 (s, 6H), 1.60–1.45 (m, 2H), 1.48–1.15 (m, 10H), 0.87 (t, 3H,  $J = 7.2$  Hz).  $^{13}\text{C}$  NMR (75 MHz,  $\text{CD}_3\text{OD}-d_4$ ):  $\delta$  (ppm) 177.2, 171.3, 168.2, 154.0, 152.1, 144.0, 142.6, 141.9, 129.6, 129.5, 127.6, 127.1, 124.9, 124.6, 124.1, 123.2, 115.1, 111.0, 104.4, 102.0, 49.7, 48.1, 44.4, 34.7, 32.9, 30.4, 30.3, 28.9, 28.4 (2C), 28.2, 27.9, 27.1, 25.6, 23.7, 14.5. HRMS (ESI-qTOF):  $m/z$   $[\text{M} + \text{H}]^+$  calcd for  $\text{C}_{36}\text{H}_{47}\text{N}_2\text{O}_2\text{S}$  572.3437, found 572.3457.

**BSA Association.** A cyanine dye solution in dimethylformamide ( $\sim 10^{-5}$  M) was used to prepare a cyanine dye solution in PBS to a final concentration of 14  $\mu\text{M}$ . To this PBS/cyanine dye solution were added different amounts of the PBS/BSA solution (14  $\mu\text{M}$ ) that were previously prepared. The final solution (2  $\mu\text{M}$  of cyanine dyes) was allowed to stand for 2 h. The apparent binding constant ( $K_a$ ) of the cyanine dyes with BSA was also obtained from fluorescence titration of the cyanine dye spectra at 25  $^\circ\text{C}$  and at constant dye concentration by dilution of the initial BSA concentration. Taking the BSA/cyanine dye association into account as 1:1,<sup>58,66</sup> the  $K_a$  could be obtained using the modified equation<sup>58,67</sup>

$$\frac{1}{(F_x - F_0)} = \frac{1}{(F_\infty - F_0)} + \frac{1}{K_a[\text{BSA}]} \frac{1}{(F_\infty - F_0)} \quad (1)$$

where  $F_0$ ,  $F_x$ , and  $F_\infty$  are the fluorescence intensities of the cyanines in the absence of BSA, in the presence of a certain amount of BSA, and at a concentration of complete interaction, respectively, and  $[\text{BSA}]$  is the protein concentration. Equation 1 can be rewritten as

$$\frac{(F_\infty - F_0)}{(F_x - F_0)} = 1 + \frac{1}{K_a[\text{BSA}]} \quad (2)$$

The binding constant values ( $K_a$ ) between the BSA and the cyanines were then calculated from the slopes of the corresponding plots  $(F_\infty - F_0)/(F_x - F_0)$  vs  $[\text{BSA}]^{-1}$ .

## ASSOCIATED CONTENT

### Supporting Information

Figures and tables giving  $^1\text{H}$  and  $^{13}\text{C}$  NMR and HRMS (ESI-MS) spectra of cyanine dyes 1–9 and photophysical data from

the BSA association study and from the cyanines in PBS. This material is available free of charge via the Internet at <http://pubs.acs.org>.

## AUTHOR INFORMATION

### Corresponding Authors

\*F.S.R.: e-mail, [fabiano.rodembusch@ufrgs.br](mailto:fabiano.rodembusch@ufrgs.br).

\*L.F.C.: tel, +55 (51) 3308 7199; fax, +55 (51) 3308 7304; e-mail, [leandra.campo@ufrgs.br](mailto:leandra.campo@ufrgs.br).

### Present Address

<sup>†</sup>Department of Chemistry, University of Miami, 1301 Memorial Drive, Miami, FL 33124-0431.

### Notes

The authors declare no competing financial interest.

## ACKNOWLEDGMENTS

The authors thank the Conselho Nacional de Desenvolvimento Científico e Tecnológico (CNPq) and the Instituto Nacional de Inovação em Diagnósticos para Saúde Pública (INDI-Saúde) for financial support.

## REFERENCES

- (1) Shindy, H. A. *Mini-Rev. Org. Chem.* **2012**, *9*, 352.
- (2) Luo, S. L.; Zhang, E. L.; Su, Y. P.; Cheng, T. M.; Shi, C. M. *Biomaterials* **2011**, *32*, 7127.
- (3) Chu, N. N.; Feng, C. L.; Ji, M. *Acta Chim. Sin. (Engl. Ed.)* **2013**, *71*, 1459.
- (4) Drummen, G. P. C. *Molecules* **2012**, *17*, 14067.
- (5) Gonçalves, M. S. T. *Chem. Rev.* **2009**, *109*, 190.
- (6) Markova, L. I.; Terpetschnig, E. A.; Patsenker, L. D. *Dyes Pigment.* **2013**, *99*, 561.
- (7) Mishra, A.; Behera, R. K.; Behera, P. K.; Mishra, B. K.; Behera, G. B. *Chem. Rev.* **2000**, *100*, 1973.
- (8) Escobedo, J. O.; Rusin, O.; Lim, S.; Strongin, R. M. *Curr. Opin. Chem. Biol.* **2010**, *14*, 64.
- (9) Yuan, L.; Lin, W.; Zheng, K.; He, L.; Huang, W. *Chem. Soc. Rev.* **2013**, *42*, 622.
- (10) El-Shishtawy, R. M. *Int. J. Photoenergy* **2009**, No. Article ID 434897.
- (11) Samanta, A.; Vendrell, M.; Das, R.; Chang, Y. T. *Chem. Commun.* **2010**, *46*, 7406.
- (12) Spittler, M. T.; Parkinson, B. A. *Acc. Chem. Res.* **2009**, *42*, 2017.
- (13) Patonay, G.; Antoine, M. D. *Anal. Chem.* **1991**, *63*, 321.
- (14) Nanjunda, R.; Owens, E. A.; Mickelson, L.; Alyabyev, S.; Kilpatrick, N.; Wang, S.; Henary, M.; Wilson, W. D. *Bioorg. Med. Chem.* **2012**, *20*, 7002.
- (15) El-Shishtawy, R. M.; Asiri, A. M.; Basaif, S. A.; Sobahi, T. R. *Spectrochim. Acta, Part A* **2010**, *75*, 1605.
- (16) Holzhauser, C.; Wagenknecht, H. A. *J. Org. Chem.* **2013**, *78*, 7373.
- (17) Volkova, K. D.; Kovalska, V. B.; Balanda, A. O.; Losytskyy, M. Y.; Golub, A. G.; Vermeij, R. J.; Subramaniam, V.; Tolmachev, O. I.; Yarmoluk, S. M. *Bioorg. Med. Chem.* **2008**, *16*, 1452.
- (18) Benzi, C.; Bertolino, C. A.; Miletto, L.; Ponzio, P.; Barolo, C.; Viscardi, G.; Coluccia, S.; Caputo, G. *Dyes Pigment.* **2009**, *83*, 111.
- (19) Bouteiller, C.; Clavé, G.; Bernardin, A.; Chipon, B.; Massoneau, M.; Renard, P. Y. *Bioconjugate Chem.* **2007**, *18*, 1303.
- (20) Haugland, R.; Cheung, C. Y.; Yue, S. US Patent Appl. US 2005191643, 2005.
- (21) Miyako, T.; Moriwaki, K. Eur. Patent Appl. EP 1496375, 2005.
- (22) Fabian, J.; Hartmann, H. *Light absorption of organic colorants*. Springer-Verlag: Berlin, Heidelberg, New York, 1980.
- (23) Tatikolov, A. S.; Costa, S. M. B. *Biophys. Chem.* **2004**, *107*, 33.
- (24) Lee, L. G.; Woo, S. L.; Head, D. F.; Dubrow, R. S.; Baer, T. M. *Cytometry* **1995**, *21*, 120.

- (25) Mader, O.; Reiner, K.; Egelhaaf, H.-J.; Fischer, R.; Brock, R. *Bioconjugate Chem.* **2004**, *15*, 70.
- (26) Pisoni, D. S.; de Abreu, M. P.; Petzhold, C. L.; Rodembusch, F. S.; Campo, L. F. *J. Photochem. Photobiol. A Chem.* **2013**, *252*, 77.
- (27) Renard, B. L.; Aubert, Y.; Asseline, U. *Tetrahedron Lett.* **2009**, *50*, 1897.
- (28) Pardal, A. C.; Ramos, S. S.; Santos, P. F.; Reis, L. V.; Almeida, P. *Molecules* **2002**, *7*, 320.
- (29) Jung, M. E.; Kim, W. J. *Bioorg. Med. Chem.* **2006**, *14*, 92.
- (30) Gerowska, M.; Hall, L.; Richardson, J.; Shelbourne, M.; Brown, T. *Tetrahedron* **2012**, *68*, 857.
- (31) Schouten, J. A.; Ladame, S.; Mason, S. J.; Cooper, M. A.; Balasubramanian, S. *J. Am. Chem. Soc.* **2003**, *125*, 5594.
- (32) Karlsson, H. J.; Lincoln, P.; Westman, G. *Bioorg. Med. Chem.* **2003**, *11*, 1035.
- (33) Rye, H. S.; Yue, S.; Wemmer, D. E.; Quesada, M. A.; Haugland, R. P.; Mathies, R. A.; Glazer, A. N. *Nucleic Acids Res.* **1992**, *11*, 2803.
- (34) Lee, L. G.; Chen, C. H.; Chiu, L. A. *Cytometry* **1986**, *7*, 508.
- (35) Svanvik, N.; Westman, G.; Wang, D.; Kubista, M. *Anal. Biochem.* **2000**, *281*, 26.
- (36) Gurrieri, S.; Wells, K. S.; Johnson, I. D.; Bustamante, C. *Anal. Biochem.* **1997**, *249*, 44.
- (37) Fujimoto, Y.; Katayama, N.; Ozaki, Y.; Yasui, S.; Iriyama, K. *J. Mol. Struct.* **1992**, *274*, 183.
- (38) Ilharco, L. M.; de Barros, R. B. *Langmuir* **2000**, *16*, 9331.
- (39) Crano, J. C.; Guglielmetti, R. *J. Organic Photochromic and Thermochromic Compounds*; Springer, 1999; Vol. 1 (Photochromic Families), p 18.
- (40) Steiger, R.; Pugin, R.; Heier, J. *Colloids Surf. B* **2009**, *74*, 484.
- (41) Khairutdinov, R. F.; Serpone, N. *J. Phys. Chem. B* **1997**, *101*, 2602.
- (42) Gadde, S.; Batchelor, E. K.; Kaifer, A. E. *Chem. Eur. J.* **2009**, *15*, 6025.
- (43) West, W.; Pearce, S. *J. Phys. Chem.* **1965**, *69*, 1894.
- (44) Kovalska, V. B.; Volkova, K. D.; Manaev, A. V.; Losytskyy, M. Y.; Okhrimenko, I. N.; Traven, V. F.; Yarmoluk, S. M. *Dyes Pigment.* **2010**, *84*, 159.
- (45) Tatikolov, A. S. *J. Photochem. Photobiol. C: Photochem. Rev.* **2012**, *13*, 55.
- (46) Carter, D. C.; Ho, J. X. *Adv. Protein Chem.* **1994**, *45*, 153.
- (47) He, H. M.; Carter, D. C. *Nature* **1992**, *358*, 209.
- (48) Peters, T. *All about Albumin: Biochemistry, Genetics, and Medical Applications*; Academic Press; Berlin, 1996.
- (49) Curry, S.; Brick, P.; Frank, N. P. *Biochim. Biophys. Acta* **1999**, *1441*, 131.
- (50) Peters, T. *Adv. Protein Chem.* **1985**, *37*, 161.
- (51) Abassi, P.; Abassi, F.; Yari, F.; Hashemi, M.; Nafisi, S. *J. Photochem. Photobiol. B: Biol.* **2013**, *122*, 61.
- (52) Sowell, J.; Agnew-Heard, K. A.; Mason, J. C.; Mama, C.; Strekowski, L.; Patonay, G. *J. Chromatogr. B* **2001**, *755*, 91.
- (53) Sowell, J.; Mason, J. C.; Strekowski, L.; Patonay, G. *Electrophoresis* **2001**, *22*, 2512.
- (54) Peyrin, E.; Guillaume, Y. C.; Guinard, C. *Biophys. J.* **1999**, *77*, 1206.
- (55) Beckford, G.; Owens, E.; Henary, M.; Patonay, G. *Talanta* **2012**, *92*, 45.
- (56) Berezin, M. Y.; Lee, H.; Akers, W.; Nikiforovich, G.; Achilefu, S. *Photochem. Photobiol.* **2007**, *83*, 1371.
- (57) Patonay, G.; Kim, J. S.; Kodagahally, R.; Strekowski, L. *Appl. Spectrosc.* **2005**, *59*, 682.
- (58) Zhang, Y. Z.; Yang, Q. F.; Du, H. Y.; Tang, Y. L.; Xu, G. Z.; Yan, W. P. *Chin. J. Chem.* **2008**, *26*, 397.
- (59) Kurtaliev, E. N. *J. Lumin.* **2012**, *132*, 2281.
- (60) Nizomov, N.; Kurtaliev, E. N.; Nizomov, S. N.; Khodjayev, G. *J. Mol. Struct.* **2009**, *936*, 199.
- (61) Kurtaliev, E. N. *J. Fluoresc.* **2011**, *21*, 1713.
- (62) Rudrawar, S.; Kondaskar, A.; Chakraborti, A. K. *Synthesis* **2005**, *15*, 2521.
- (63) Bayo, K.; Bayo-Bangoura, M.; Mossoyan-Deneux, M.; Lexa, D.; Ouedraogo, G. V. C. *R. Chim.* **2007**, *10*, 482.
- (64) Savolainen, J.; van der Linden, D.; Dijkhuizen, N.; Herek, J. L. *J. Photochem. Photobiol. A: Chem.* **2008**, *196*, 99.
- (65) Würth, C.; Grabolle, M.; Pauli, J.; Spieles, M.; Resch-Genger, U. *Nat. Protoc.* **2013**, *8*, 1535.
- (66) Tatikolov, A. S.; Costa, S. M. B. *Biophys. Chem.* **2004**, *107*, 33.
- (67) Benesi, H. A.; Hildebrand, J. H. *J. Am. Chem. Soc.* **1949**, *71*, 2703.